Journal of Molecular Structure 1236 (2021) 130317

Contents lists available at ScienceDirect

Journal of Molecular Structure

journal homepage: www.elsevier.com/locate/molstr

Design, synthesis, antiproliferative evaluation, and molecular docking study of new quinoxaline derivatives as apoptotic inducers and EGFR inhibitors

Eman A. Fayed[a,*], Yousry A. Ammar[b,*], Marwa A. Saleh[a], Ashraf H. Bayoumi[c], Amany Belal[d,e], Ahmed B.M. Mehany[f], Ahmed Ragab[b,*]

[a] Pharmaceutical Organic Chemistry Department, Faculty of Pharmacy (Girls), Al-Azhar University, Nasr City, Cairo, 11754, Egypt
[b] Chemistry Department, Faculty of Science (Boys), Al-Azhar University, Nasr City, Cairo, 11884, Egypt
[c] Pharmaceutical Organic Chemistry Department, Faculty of Pharmacy (Boys), Al-Azhar University, Nasr City, Cairo, 11754, Egypt
[d] Department of Pharmaceutical Chemistry, College of Pharmacy, Taif University, P.O. Box 11099, Taif, 21944, Saudi Arabia
[e] Medicinal Chemistry Department, Faculty of Pharmacy, Beni-Suef University, Beni-Suef, 62514, Egypt
[f] Zoology Department, Faculty of Science, Al-Azhar University, Nasr City, Cairo, 11884, Egypt

ARTICLE INFO

Article history:
Received 21 October 2020
Revised 15 March 2021
Accepted 16 March 2021
Available online 22 March 2021

Keywords:
Quinoxaline
Anticancer activity
Apoptosis
EGFR inhibitor
Molecular docking simulation

ABSTRACT

A new series of quinoxaline derivatives synthesized and pharmacologically evaluated against (HepG-2, HCT-116, and MCF-7) cell lines. Seven compounds were found to possess the highest activities against the examined cell lines with IC_{50} values ranging from (7.57 to 28.44 μM). To further analyze its apoptotic potential in MCF-7 cells, the most active **3a, 3b, 6, 7b, 7c, 7d**, and **7f** members have been selected. Interestingly, it found that the Bcl-2 level decreased by 1.95–3.99 folds, and the BAX level increased by 7.2-10.6 folds relative to the control. They also increased the active Caspase-3 level by 5.77-10.69 folds compared to untreated cells. WI38 cells were treated with these compounds to estimate the cytotoxicity level of those compounds in non-tumorigenic cells, and they displayed higher IC_{50} values (142.21-335.03μM), suggesting may less toxic effect on the normal ones. Further studies on the mechanism of the most promising compounds **3a, 6, 7b** and **7d**, revealed that it increases apoptotic cells and induced cell cycle arrest at pre-G1 and G2/M phases. Besides, both wild $EGFR^{WT}$ and mutant $EGFR^{L858R-TK}$ inhibitory activity for these derivatives showed that these derivatives had IC_{50} values ranging from 0.075-1.547 μM versus wild $EGFR^{WT}$ and 63.70-87.34 nM versus the mutant type. Erlotinib was used as a standard reference with IC_{50} values of 0.0656 μM and 59.56 nM versus both types. Finally, the molecular docking study of most potent quinoxaline derivatives exhibited a good binding inside the active site of EGFR (1M17), with binding energy ranged between (-15.86 to -16.97) compared to Erlotinib (-17.84) kcal/mol. Also, by applying Lipinski's parameters, it was found that these derivatives showed no violations and indicated promiscuity to formulate orally.

1. Introduction

As one of the most serious clinical conditions, cancer continues to endanger people's health all over the world [1,2]. Cancer cannot be identified as a single disease and can only represent a large group of malignant cells differentiated from healthy cells by uncontrolled growth due to a severe disorder of the cell cycle's regulatory system [3]. Cancer of the lung, stomach, breast, and melanoma is the most prevalent in developed and developing countries. The application of chemotherapy has been a frequently preferred, effective way of treating cancer. Cytotoxic agents and antihormonal drugs are the principal chemotherapeutics that reduce malignant cell proliferation. On the other hand, significant side effects such as nausea, vomiting, diarrhea, hair loss, severe infections, and tumor-cell population growth are frequently encountered during chemotherapy [4–7]. Therefore, significant chemotherapy progress would require new and useful antitumor agents to eradicate the entire range of cancer diseases worldwide with greater efficacy and lower side effects. DNA-damaging agents such as radiation and chemotherapy drugs may cause cell death (apoptosis) that is programmed. Studies have shown a strong link between increased drug resistance to cancer and reduced apoptosis

* Corresponding authors.
E-mail addresses: alfayed_e@azhar.edu.eg (E.A. Fayed), yossry@yahoo.com (Y.A. Ammar), ahmed_ragab@azhar.edu.eg (A. Ragab).

https://doi.org/10.1016/j.molstruc.2021.130317
0022-2860/

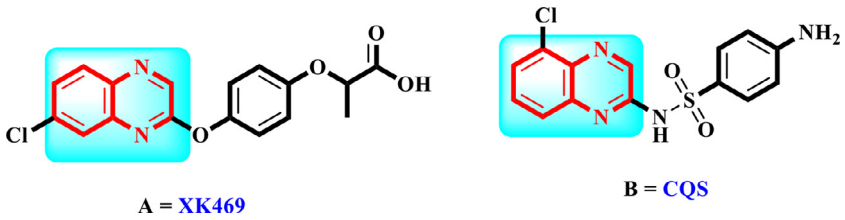

A = XK469 B = CQS

Fig. 1. Molecular structure of the antineoplastic lead compounds XK469 and CQS.

capacity [8]. The susceptibility to apoptosis is thus a significant determinant of the response to antineoplastic therapy [9]. Therefore, apoptosis inhibition will play a major role in the progression of cancer during carcinogenesis. There are various types of molecular pathways used by cancer cells to inhibit apoptosis. They acquire apoptosis resistance by expressing anti-apoptotic proteins such as Bcl-2 or by the down-regulation of various caspases and pro-apoptotic proteins such as BAX [10]. A significant determinant of cell survival is the relationship between the pro-apoptotic and anti-apoptotic levels [11].

Besides, the receptor of the Epidermal Growth Factor (EGFR) is a transmembrane glycoprotein tyrosine kinase receptor that is overexpressed in many cancer cells such as (breast, ovarian, and human colon cancers) [12]. Over-expression of the EGFR family results in autophosphorylation of several tyrosine residues within the receptor COOH-terminal tail, which initiates a certain cascade resulting in cell proliferation, differentiation, and anti-apoptosis. Thus inhibition of the EGFR family has been identified as having an important role in developing targeted chemotherapeutic agents [12]. Quinoxalines have been reported as candidates for treating cancer and disorders associated with angiogenesis functions [13–18].

For example, 2-(4-(7-chloroquinoxalin-2-yl)phenoxy]propionic acid (XK469) (**A**) and chloroquinoxalinesulfonamide (CQS) (**B**) are known as antineoplastic quinoxalines (Fig. 1). There are also some naturally occurring *bis*-quinoxaline compounds known as antitumor antibiotics. Triostin A, Azatriostin, and Echinomycin, which displayed antitumor activity, are the leading examples of this antineoplastic group [19–25].

Also, dihydroquinoxalin-2-ones and their derivatives are an important structural motive for biologically active compounds discovery [26–29]. Quinoxaline-2-carboxylic acid is also a fragment of the Echinomycin and Triostin antibiotics, a powerful active anticancer agent [30]. The quinoxaline-2-carboxylic acid chromophore moiety plays an important biogenetic role in antibiotic triostion synthesis [30].Quinoxaline-2-carboxylic acid derivative (Quinacillin) is a Penicillin-related semi-synthetic antibiotic [30,31]. On the other hand, hydrazide-hydrazones have been reported to have anticancer activity [32–35] and have been described as interesting privileged structures, being largely used in the design of new bioactive compounds with distinct pharmacological profiles, such as antitrypanosome [36–40]. Because of these facts, and as part of our ongoing interest in anticancer activity [41–45]. Herein, we report the synthesis of new quinoxaline derivatives incorporating various ester and hydrazide moieties and hoping to be exhibited a proper screening for their and anticancer activities. The reason for such a study stemmed from the great importance and synthetic accessibility of the quinoxaline ring in generating potential anticancer molecules. The newly synthesized compounds are structurally related to certain biologically active molecules, besides multiple esters and hydrazide fragments bearing the quinoxaline moiety as essential pharmacophores and varying lipophilicity degrees. Nowadays, the development of hybrid molecules is a trend that aims to combine multiple pharmacophore fragments in the same structure with different biological potentials [46–56] (Fig. 2).

2. Experimental

2.1. Chemistry

All melting points were taken on Electrothermal LA 9000 SERIS, Digital Melting point Apparatus, and were uncorrected. IR Spectra were determined using the KBr disc technique on Nikolet IR 200 FT IR Spectrophotometer at Pharmaceutical Analytical Unit, Faculty of Pharmacy, Al-Azhar University, and on Cary IR 630 FT IR spectrophotometer at Analytical Unit, Faculty of Science (boys), Al-Azhar University and values are represented in cm^{-1}. The ^{1}H NMR and ^{13} C NMR spectra were recorded on Gemini Mercury 400 MHz NMR spectrometer at the Main Chemical Warfare Laboratories, Chemical Warfare Department, Ministry of Defense. DMSO-d_6 was used as a solvent; chemical shifts were measured in δ ppm, relative to TMS as an internal standard. Mass spectra were recorded at 70 ev on DI-50 unit of Schimadzu GC/ MS-QP5050A Spectrometer at Regional Center for Mycology and Biotechnology, Al-Azhar University. Microanalysis was carried out at Regional Center for Mycology and Biotechnology, Al-Azhar University. Anticancer activity was carried out in local strain identified in Regional Center for genetic engineering, faculty of Science (boys), Al-Azhar University, and BAX, Bcl-2 and EGFR both wide and mutant were carried out in (VACSERA), Cairo, Egypt. Progress of the reaction was monitored by using TLC sheets pre-coated with UV fluorescent silica gel Merck 60F254 plates and were visualized using a UV lamp. Solvent for TLC: Hexane: Ethyl acetate in ratio 6:4 and 4:6.

Methyl 2-(3-oxo-3,4-dihydroquinoxalin-2(1*H*)-ylidene)acetate derivatives (2a-c)

A mixture of *O*-phenylenediamine derivatives **(1)** (0.01 mol) and dimethyl acetylene dicarboxylate (0.01mol) in ethanol (20 mL) was stirred for half an hour at room temperature, then the separated solid filtered and crystallized from ethanol.

Methyl-2-(6-bromo-3-oxo-3,4-dihydroquinoxalin-2(1*H*)-ylidene)acetate (2a)

Light brown powder; Yield: (89%); m.p.: 200-202°C; IR (KBr, cm^{-1})= 3218 (NH), 3068 (CH-arom), 2947, 2843 (CH-aliph), 1694 (C=O), 1652 (C=O; amide), 1627 (C=N); ^{1}H NMR (400 MHz, DMSO-d_6) δ/ppm 3.66 (s, 3H, OCH_3), 5.53 (s, 1H, CH-vinylic), 7.15 (d, J = 8.4 Hz, 1H, Ar-H), 7.19 (dd, J = 8.8, 2.0 Hz, 1H, Ar-H), 7.41 (d, J = 8.4 Hz, 1H, Ar-H), 10.99, 11.76 (2s, 2H, 2NH exchangeable by D_2O), ^{13}C NMR (100 MHz, DMSO-d_6) δ/ppm 51.24 (OCH_3), 84.85 (CH-vinylic), 113.94, 117.70, 118.37, 124.87, 126.24, 127.15, 143.73 (C=N), 155.85, 169.60 (2C=O); MS (EI, 70 eV): m/z (%)= 299 [M^{+2}] (21.82%), 297 [$M^{\cdot+}$] (10.58%), 265 (100%); Anal. Calc. for $C_{11}H_9BrN_2O_3$ (297.11): C, 44.47; H, 3.05; N, 9.43. Found: C, 44.36; H, 3.10; N, 9.23.

Methyl-2-(6-chloro-3-oxo-3,4-dihydroquinoxalin-2(1*H*)-ylidene)acetate (2b)

Deep brown powder; Yield: (97%); m.p.: 220-222°C; IR (KBr, cm^{-1}) = 3218 (NH), 3074 (CH-arom), 2948, 2860 (CH-aliph), 1693 (C=O-ester; hydrogen bond), 1652 (C=O-amide); ^{1}H NMR (400 MHz, DMSO-d_6) δ/ppm 3.67 (s, 3H, OCH_3), 5.54 (s, 1H, CH-vinylic), 7.08 (d, J = 8.4 Hz, 1H, Ar-H), 7.33 (dd, J = 8.8, 2.0 Hz, 1H, Ar-H), 7.75 (d, J = 8.8 Hz, 1H, Ar-H), 10.99, 11.77 (2s, 2H, 2NH ex-

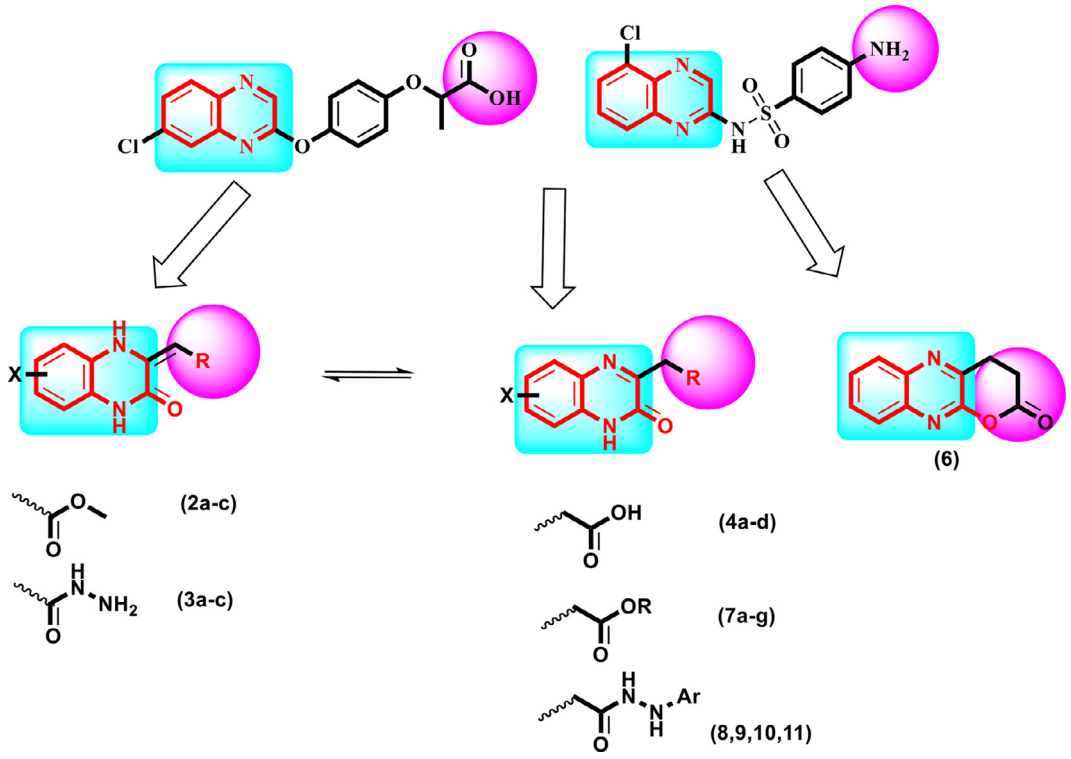

Fig. 2. Quinoxaline hybrids with ester and hydrazide moieties.

changeable by D_2O); ^{13}C NMR (100 MHz, DMSO-d_6) δ/ppm 51.23 (OCH_3), 84.75 (CH-vinylic), 114.90, 117.45, 123.44, 124.50, 126.84, 130.49, 143.74 (C=N), 156.02, 169.83 (2C=O); MS (EI, 70 eV): *m/z* (%)= 254 [M^{+2}] (35.16%), 252 [$M^{\cdot+}$] (16.84%), 43 (100%); Anal. Calc. for $C_{11}H_9ClN_2O_3$ (252.65): C, 52.29; H, 3.59; N, 11.09; Found: C, 52.18; H, 3.49; N, 11.12.

Methyl-2-(7-benzoyl-3-oxo-3,4-dihydroquinoxalin-2(1*H*)-ylidene)acetate (2c)

Light yellow powder; Yield: (92%); m.p.: 185-187°C; IR (KBr, cm^{-1})= 3232 (NH), 3076 (CH-arom), 2946, 2840 (CH-aliph), 1698 (C=O-ester; hydrogen bond), 1658, (C=O), 1605 (C=N); ^1H NMR (400 MHz, $CDCl_3$) δ/ppm 3.78 (s, 3H, OCH_3), 5.88 (s, 1H, CH-vinylic), 6.70 (d, J = 8.0 Hz, 1H, Ar-H), 7.12 (d, J = 8.0 Hz, 1H, Ar-H), 7.47 (t, J = 7.6 Hz, 2H, Ar-H), 7.51 (dd, J = 6.4, 1.6 Hz, 1H, Ar-H), 7.63 (t, J = 7.4 Hz, 1H, Ar-H), 7.74 (d, J = 7.2 Hz, 1H, Ar-H), 7.77 (d, J = 6.8 Hz, 1H, Ar-H), 11.16, 10.22 (s, 2H, 2NH exchangeable by D_2O); ^{13}C NMR (100 MHz, $CDCl_3$): δ 51.30 (OCH_3), 87.17 (CH-vinylic), 114.41, 119.08, 124.88, 125.42, 127.99, 128.42, 129.57, 129.77, 131.39, 132.48, 138.83, 140.77, 142.75 (C=N), 157.49, 170.71, 194.96 (3C=O); MS (EI, 70 eV): *m/z* (%) = 322 [M^+] (100 %); Anal. Calc. for $C_{18}H_{14}N_2O_4$ (322.32): C, 67.08; H, 4.38; N, 8.69; Found: C, 66.80; H, 4.35; N, 8.65.

2-(3-Oxo-3,4-dihydroquinoxalin-2-yl)acetohydrazide derivatives (3a- c)

A mixture of the quinoxaline acetate ester **2a-c** (0.01mol) and hydrazine hydrate (0.05mol) was heated under reflux condition in ethanol (10 mL) for 6 h; the separated solid filtered off and crystallized from benzene.

2-(6-Bromo-3-oxo-3,4-dihydroquinoxalin-2(1*H*)-ylidene) acetohydrazide (3a)

Light brown powder; Yield: (88)%; m.p.: 280-282°C; IR (KBr, cm^{-1})= 3322, 3254 (br-NH_2 & NH), 3055 (CH-arom), 2942 (CH-aliph), 1684 (C=O), 1603 (C=N); ^1H NMR (400 MHz, DMSO-d_6) δ/ppm 4.36 (s, 2H, NH_2 exchangeable by D_2O), 5.62 (s, 1H, CH-vinylic), 6.91 (d, J = 8.4 Hz, 1H, Ar-H), 7.11 (s, H, NH exchangeable by D_2O) 7.44 (s, 1H, Ar-H), 7.64 (d, J = 8.4 Hz, 1H, Ar-H), 9.20, 11.62 (2s, 2H, 2NH exchangeable by D_2O); ^{13}C NMR (101 MHz, DMSO-d_6) δ/ppm 115.16, 116.92, 122.52, 123.95, 126.32, 130.66, 134.77, 154.42 (N-C=C), 161.32, 164.61(2C=O); MS (EI, 70 eV): *m/z* (%)= 299 [M^{+2}] (26.85%), 297 [$M^{\cdot+}$] (24.67%), 293 (100%); Anal. Calc. for $C_{10}H_9BrN_4O_2$ (297.11): C, 40.43; H, 3.05; N, 18.86; Found: C, 40.33; H, 3.02; N, 18.66.

2-(6-Chloro-3-oxo-3,4-dihydroquinoxalin-2(1*H*)-ylidene) acetohydrazide (3b)

Black powder; Yield: (92) %; m.p.: >300°C; IR (KBr, cm^{-1})= 3429, 3316, 3276 (NH_2 & NH), 3067 (CH-arom), 2921, 2852 (CH-aliph), 1674 (br. C=O), 1609 (C=N); ^1H NMR (400 MHz, DMSO-d_6): δ/ppm 4.43 (s, 2H, NH_2 exchangeable by D_2O), 5.60 (s, 1H, CH-vinylic), 6.96 (d, J = 8.4 Hz, 1H, Ar-H), 6.98 (s, 1H, NH, exchangeable by D_2O), 7.17 (d, J = 8.8 Hz, 1H, Ar-H), 7.29 (s, 1H, Ar-H), 9.19, 11.61 (2s, 2H, 2NH exchangeable by D_2O); ^{13}C NMR (101 MHz, DMSO) δ 114.52, 117.42, 122.09, 126.14, 130.23, 131.23, 132.22, 154.48 (N-C=C), 161.22, 165.65 (2C=O); MS (EI, 70 eV): *m/z* (%)= 254 [M^{+2}] (30.24%), 252 [$M^{\cdot+}$] (79.31%), 220 (100%); Anal. Calc. for $C_{10}H_9ClN_4O_2$ (252.66): C, 47.54; H, 3.59; N, 22.18; Found: C, 47.20; H, 3.47; N, 22.22.

2-(7-Benzoyl-3-oxo-3,4-dihydroquinoxalin-2(1*H*)-ylidene) acetohydrazide (3c)

Light brown powder; Yield: (74) %; m.p.: 280-282°C; IR (KBr, cm^{-1})= 3288, 3200 (br. NH_2 & 2NH), 3054 (CH-arom), 2922, 2861 (CH-aliph), 1674 (br. C=O), 1609 (C=N); ^1H NMR (400 MHz, DMSO-d_6) δ/ppm 4.28 (s, 2H, NH_2 exchangeable by D_2O), 5.56 (s, 1H, CH-vinylic), 6.92 (s, 1H, NH, exchangeable by D_2O), 7.22 (t, J = 6.8 Hz, 2H, Ar-H), 7.27 (d, J = 8.2 Hz, 2H, Ar-H), 7.36 (d, J = 7.2 Hz, 1H, Ar-H), 7.50 (t, J = 7.2 Hz, 1H, Ar-H), 7.55 (d, J = 8.0 Hz, 1H, Ar-H), 7.59 (s, 1H, Ar-H), 9.13, 11.58 (2s, 2H, 2NH exchangeable by D_2O); ^{13}C NMR (101 MHz, DMSO) δ/ppm 106.98, 114.46, 117.76, 119.58, 121.85, 128.59, 129.36, 129.47, 133.06, 133.96, 135.44,

137.27, 139.31, 157.01 (N-C=C), 162.13, 165.81, 184.05 (3C=O); MS (EI, 70 eV): *m/z* (%)= 322 [M·+] (31.44%), 52 (100%); Anal. Calc. for $C_{17}H_{14}N_4O_3$ (322.32): C, 63.35; H, 4.38; N, 17.38; Found: C, 62.98; H, 4.27; N, 17.28.

3-(3-Oxo-3,4-dihydroquinoxalin-2-yl)propanoic acid derivatives (4a-d)

O-Phenylenediamines (0.01 mol), and α-ketoglutaric acid (0.01mol) in acetic acid (20 mL) have stirred for 30 min., at room temperature, and then the solid that obtained was collected by filtration and recrystallized from methanol.

3-(3-Oxo-3,4-dihydroquinoxalin-2-yl)propanoic acid (4a): m.p: 255-258 °C [57]

3-(6-Bromo-3-oxo-3,4-dihydroquinoxalin-2-yl)propanoic acid (4b)

Deep brown powder; Yield: (70%); m.p: >300°C; IR (KBr, cm^{-1})= 3413(OH-carboxylic), 3150 (NH), 3064 (CH-arom), 2997, 2930, 2860 (CH-aliph), 1689, 1670 (2C=O), 1603 (C=N); ^{1}H NMR (400 MHz, DMSO-d_6) δ/ppm 2.68 (t, J = 7.0 Hz, 2H, CH_2), 2.98 (t, J = 7.0 Hz, 2H, CH_2), 7.21 (d, J = 8.8 Hz, 1H, Ar-H), 7.40 (s, 1H, Ar-H), 7.60 (d, J = 8.0 Hz, 1H, Ar-H), 12.36, 12.42 (2*s*, 2H, NH, OH exchangeable by D_2O); ^{13}C NMR (100 MHz, DMSO-d_6) δ/ppm 28.12, 29.90 ($2CH_2$), 117.93, 122.32, 126.37, 130.34, 130.87, 133.41, 154.71 (C=N), 161.45, 174.24 (2C=O); MS (EI, 70 eV): *m/z* (%) = 299 [M^{+2}] (3.78%), 297 [M·+] (4.75%), 252 (100%); Anal. Calc. for $C_{11}H_9BrN_2O_3$ (297.11): C, 44.47; H, 3.05; N, 9.43; Found: C, 44.23; H, 2.95; N, 9.31.

3-(6-Chloro-3-oxo-3,4-dihydroquinoxalin-2-yl)propanoic acid (4c) [58]

Deep violet powder; Yield: (76%); m.p: 260-262°C; IR (KBr, cm^{-1})= 3425 (OH), 3156 (NH), 3068 (CH-arom), 2973, 2864 (CH-aliph), 1690, 1665 (2C=O), 1606(C=N); ^{1}H NMR (400 MHz, DMSO-d_6) δ/ppm 2.70 (t, J = 7.0 Hz, 2H, CH_2), 2.99 (t, J = 6.8 Hz, 2H, CH_2), 7.27 (d, J = 8.8 Hz, 1H, Ar-H), 7.52 (dd, J = 8.4, 2.4 Hz, 1H, Ar-H), 7.67 (d, J = 7.6 Hz, 1H, Ar-H), 12.38, 12.42 (2s, 2H, NH, OH exchangeable by D_2O); ^{13}C NMR (100 MHz, DMSO-d_6) δ/ppm 27.64, 29.48 ($2CH_2$), 114.51, 123.13, 127.05, 129.73, 131.98, 133.41, 154.32 (C=N), 160.82, 173.81 (2C=O); MS (EI, 70 eV): *m/z* (%)= 254 [M^{+2}] (33.19%), 252 [M^+] (100%); Anal. Calc. for $C_{11}H_9ClN_2O_3$ (252.65): C, 52.29; H, 3.59; N, 11.09; Found: C, 52.43; H, 3.68; N, 10.93.

3-(7-Benzoyl-3-oxo-3,4-dihydroquinoxalin-2-yl)propanoic acid (4d)

Light yellow powder; Yield: (80%); m.p: 230-232°C; IR (KBr, cm^{-1})= 3475 (br -OH), 3139 (NH), 3006 (CH-arom), 2916, 2850 (CH-aliph), 1693, 1657, (C=O), 1612 (C=N); ^{1}H NMR (400 MHz, DMSO-d_6) δ/ppm 2.71 (t, J = 7.0 Hz, 2H, CH_2), 3.03 (t, J = 7.0 Hz, 2H, CH_2), 7.42 (d, J = 8.4 Hz, 1H, Ar-H), 7.59 (t, J = 7.6 Hz, 2H, Ar-H), 7.69 (t, J = 7.4 Hz, 1H, Ar-H), 7.74 (d, J = 7.2 Hz, 2H, Ar-H), 7.91 (dd, J = 8.4, 2.0 Hz, 1H, Ar-H), 7.95 (d, J = 8.0 Hz, 1H, Ar-H), 12.07, 12.65 (2s, 2H, NH, OH exchangeable by D_2O); ^{13}C NMR (100 MHz, DMSO-d_6) δ/ppm 28.29, 29.66 ($2CH_2$), 108.76, 114.86, 116.36, 119.01, 122.45, 124.65, 127.70, 129.63, 131.28, 133.57, 134.47, 140.56, 151.78 (C=N), 155.22, 179.53, 191.77 (3C=O); MS (EI, 70 eV): *m/z* (%)= 322 [M·+] (100 %); Anal. Calc. for $C_{18}H_{14}N_2O_4$ (322.32): C, 67.08; H, 4.38; N, 8.69; Found: C, 67.25; H, 4.70; N, 8.89.

3,4-Dihydro-2*H*-pyrano[2,3-*b*]quinoxalin-2-one (6):

To a solution of 3-(3-oxo-3,4-dihydroquinoxalin-2-yl)propanoic acid **(4a)** (0.01 mol) and excess $SOCl_2$ (5 mL) in dry benzene (10 mL) was heated under reflux for 4 h, with continuous stirring, then the reaction mixture cooled and the solid product collected and recrystallized from ethanol.

Deep green powder; Yield: (82%); m.p: 220-222°C, IR (KBr, cm^{-1})= 3050 (CH-arom), 2911, 2887, 2818 (CH-aliph), 1688 (C=O), 1605 (C=N); ^{1}H NMR (400 MHz, DMSO-d_6) δ/ppm 2.70 (t, J = 6.8 Hz, 2H, CH_2), 2.99 (t, J = 7.0 Hz, 2H, CH_2), 7.26 (t, J = 6.8 Hz, 1H, Ar-H), 7.28 (d, J = 8.0 Hz, 1H, Ar-H), 7.47 (t, J = 7.2 Hz, 1H, Ar-H), 7.67 (d, J = 8.0 Hz, 1H, Ar-H); ^{13}C NMR (100 MHz, DMSO-d_6) δ/ppm 28.08, 30.03 ($2CH_2$), 115.68, 123.50, 128.50, 129.87, 131.91, 132.10, 155.00, 160.69 (2C=N), 174.31 (C=O); MS (EI, 70 eV): *m/z* (%)= 200 [M^+] (10.74 %), 41 (100%); Anal. Calc. for $C_{11}H_8N_2O_2$ (200.20): C, 66.00; H, 4.03; N, 13.99; Found: C, 66.06; H, 4.03; N, 13.97.

Methyl or ethyl 3-(3-oxo-3,4-dihydroquinoxalin-2-yl)propa tnoate derivatives (7a-g)

To a solution of **4** (0.01mol) in methanol or ethanol (10 mL), concentrated sulfuric acid (1 mL) has added. The reaction mixture was heated under reflux for 3 h, then the solution was allowed to be cooled, then the ester products were collected by filtration.

Ethyl 3-(3-oxo-3,4-dihydroquinoxalin-2-yl)propanoate (7a) [59]

Methyl 3-(6-bromo-3-oxo-3,4-dihydroquinoxalin-2-yl)propa noate (7b) [60]

Black shiny crystals; Yield (56%); m.p: 200-202°C; IR (KBr, cm^{-1})= 3445 (NH), 3066 (CH-arom), 2946, 2843 (CH-aliph), 1730 (C=O-ester), 1666 (CO-amide), 1606 (C=N); ^{1}H NMR (400 MHz, DMSO-d_6) δ/ppm 2.78 (t, J = 7.0 Hz, 2H, CH_2), 3.04 (t, J = 6.8 Hz, 2H, CH_2), 3.59 (s, 3H, OCH_3), 7.41 (d, J = 8.4 Hz, 1H, Ar-H), 7.42(s, 1H, Ar-H), 7.60 (d, J = 8.4 Hz, 1H, Ar-H), 12.39 (s, 1H, NH exchangeable by D_2O); MS (EI, 70 eV): *m/z* (%)= 313 [M^{+2}] (5.07%), 311 [M^+] (3.32%), 277 (100%); Anal. Calc. for $C_{12}H_{11}BrN_2O_3$ (311.14): C, 46.32; H, 3.56; N, 9.00; Found: C, 46.70; H, 3.58; N, 8.87.

Ethyl-3-(6-bromo-3-oxo-3,4-dihydroquinoxalin-2-yl)propa noate (7c)

Dark green crystals; Yield: (87%); m.p: 170-172°C; IR (KBr, cm^{-1}) = 3442 (NH), 3052 (CH-arom), 2941, 2856 (CH-aliph), 1725 (C=O-ester), 1662 (C=O-amide), 1605 (C=N); ^{1}H NMR (400 MHz, DMSO-d_6): δ/ppm 1.07 (t, J = 7.0 Hz, 3H, CH_2-$\underline{CH_3}$), 2.78 (t, J = 7.0 Hz, 2H, CH_2),), 3.05 (t, J = 6.8 Hz, 2H, CH_2), 4.12 (q, J = 7.6 Hz, 2H, $\underline{CH_2}$-CH_3), 7.27 (s, 1H, Ar-H), 7.30 (d, 1H, Ar-H), 7.68 (d, J = 8.0 Hz, 1H, Ar-H), 12.41 (s, 1H, NH exchangeable by D_2O); ^{13}C NMR (100 MHz, DMSO-d_6) δ/ppm 15.42 (CH_3), 27.20, 29.37 ($2CH_2$), 61.39 (OCH_2), 112.57, 113.13, 119.50, 124.88, 130.08, 136.66, 149.95 (C=N), 164.23, 173.28 (2C=O); MS (EI, 70 eV): *m/z* (%)= 327 [M^{+2}] (5.82%), 325 [M·+] (8.23%), 251 (100%); Anal. Calc. for $C_{13}H_{13}BrN_2O_3$ (325.16): C, 48.02; H, 4.03; N, 8.62; Found: C, 47.85; H, 3.67; N, 8.40.

Methyl-3-(6-chloro-3-oxo-3,4-dihydroquinoxalin-2-yl)propa noate (7d) [58]

Black shiny crystals; Yield: (50%); m.p.: 190-192°C; IR (KBr, cm^{-1})= 3453 (NH), 3068 (CH-arom), 2948, 2845 (CH-aliph), 1733 (C=O-ester), 1665 (CO-amide), 1612 (C=N); ^{1}H NMR (400 MHz, DMSO-d_6) δ/ppm 2.95 (t, J = 7.0 Hz, 2H, CH_2), 3.21 (t, J = 6.8 Hz, 2H, CH_2), 3.76 (s, 3H, OCH_3), 7.45 (d, J = 7.6 Hz, 1H, Ar-H), 7.68 (s, 1H, Ar-H), 7.84 (d, J = 8.0 Hz, 1H, Ar-H), 12.58 (s, 1H, NH exchangeable by D_2O); MS (EI, 70 eV): *m/z* (%)= 268 [M^{+2}] (33.64%), 266 [M^+] (100%); Anal. Calc. for $C_{12}H_{11}ClN_2O_3$ (266.68): C, 54.05; H, 4.16; N, 10.50; Found: C, 54.13; H, 4.02; N, 10.92.

Ethyl 3-(6-chloro-3-oxo-3,4-dihydroquinoxalin-2-yl)propa noate (7e)

Deep green crystals; Yield: (87%); m.p.: 160-162°C; IR (KBr, cm^{-1})= 3431 (NH), 3050 (CH-arom), 2987, 2867 (CH-aliph), 1735 (C=O-ester), 1664 (CO-amide), 1616 (C=N); ^{1}H NMR (400 MHz, DMSO-d_6) δ/ppm 1.16 (t, J = 7.0 Hz, 3H, CH_2-$\underline{CH_3}$), 2.74 (t, J = 7.0 Hz, 2H, CH_2), 3.02 (t, J = 7.0 Hz, 2H, CH_2), 4.06 (q, J = 7.1 Hz, 2H, $\underline{CH_2}$-CH_3), 7.29 d, J = 7.0 Hz, 1H, Ar-H), 7.26 (s, 1H, Ar-H), 7.65 (d, J = 7.1 Hz, 1H, Ar-H), 12.39 (s, 1H, NH exchangeable by D_2O); ^{13}C NMR (101 MHz, DMSO) δ/ppm 14.60 (CH_2-$\underline{CH_3}$), 28.12, 29.90 (2 CH_2), 60.73 ($\underline{CH_2}$-CH_3), 117.93, 122.32, 126.37, 130.87, 132.45, 133.41, 154.71 (C=N), 161.45, 174.24 (2C=O); MS (EI, 70 eV): *m/z* (%)= 282 [M^{+2}] (2.87%), 280 [M·+] (8.88%), 110 (100%); Anal. Calc. for $C_{13}H_{13}ClN_2O_3$ (280.71): C, 55.62; H, 4.67; N, 9.98; Found: C, 55.83; H, 5.03; N, 9.74.

Methyl-3-(7-benzoyl-3-oxo-3,4-dihydroquinoxalin-2-yl)propanoate (7f)

Deep brown powder; Yield: (66%); m.p.: 110-112°C; IR (KBr, cm^{-1})= 3230 (NH), 3087 (CH-arom), 2967, 2927, 2885 (CH-aliph), 1735 (C=O-ester), 1678, 1655 (2C=O), 1608 (C=N); ^{1}H NMR (400 MHz, DMSO-d_6) δ/ppm 2.77 (t, J = 7.0 Hz, 2H), 3.04 (t, J = 7.0 Hz, 2H), 3.55 (s, 3H, OCH_3), 7.41 (d, J = 8.4 Hz, 1H, Ar-H), 7.57 (t, J = 7.4 Hz, 2H, Ar-H), 7.68 (t, J = 6.8 Hz, 1H, Ar-H), 7.72 (d, J = 8.0 Hz, 2H, Ar-H), 7.89 (d, J = 8.4 Hz, 1H, Ar-H), 7.90 (s, 1H, Ar-H), 12.62 (s, 1H, NH exchangeable by D_2O); ^{13}C NMR (100 MHz, DMSO-d_6) δ/ppm 27.51, 29.32 ($2CH_2$), 51.24(OCH_3), 118.13, 124.44, 127.01, 129.44, 129.68, 130.28, 133.77, 134.13, 138.33, 147.69, 155.35 (C=N), 160.61, 179.18, 194.28 (3C=O); MS (EI, 70 eV): m/z (%)= 336 [M·$^+$] (16.64%), 304 (100%); Anal. Calc. for $C_{19}H_{16}N_2O_4$ (336.35): C, 67.85; H, 4.80; N, 8.33; Found: C, 68.10; H, 4.62; N, 8.14.

Ethyl 3-(7-benzoyl-3-oxo-3,4-dihydroquinoxalin-2-yl)propanoate (7g)

Pale brown crystals; Yield: (85%); m.p.: 140-142°C; IR (KBr, cm^{-1}) = 3228 (NH), 3065 (CH-arom), 2991, 2850 (CH-aliph), 1711 (C=O-ester), 1677, 1651 (2C=O), 1610 (C=N); ^{1}H NMR (400 MHz, DMSO-d_6) δ/ppm 1.12 (t, J = 7.2 Hz, 3H, CH_2-$\underline{CH_3}$), 2.74 (t, J = 6.8 Hz, 2H, CH_2), 3.06 (t, J = 6.8 Hz, 2H, CH_2), 4.04 (q, J = 7.2 Hz, 2H, $\underline{CH_2}$-CH_3), 7.42 (d, J = 8.8 Hz, 1H, Ar-H), 7.58 (t, J = 7.4 Hz, 2H, Ar-H), 7.69 (t, J = 7.4 Hz, 1H, Ar-H), 7.70 (d, 1H, Ar-H), 7.72 (s, 1H, Ar-H), 7.91 (d, J = 7.2 Hz, 2H, Ar-H), 12.66 (s, 1H, NH exchangeable by D_2O), ^{13}C NMR (100 MHz, DMSO-d_6) δ/ppm 14.56 (CH_3), 28.08, 29.86 ($2CH_2$), 60.22 (OCH_2), 116.22, 129.01, 129.80, 130.79, 131.99, 132.90, 135.68, 137.72, 155.06 (C=N), 161.87, 172.79, 194.80 (3C=O); MS (EI, 70 eV): m/z (%)= 350 [M·$^+$] (78.16%), 277 (100%); Anal. Calc. for $C_{20}H_{18}N_2O_4$ (350.37): C, 68.56; H, 5.18; N, 8.00; Found: C, 68.28; H, 4.89; N, 7.85.

3-(3-Oxo-3,4-dihydroquinoxalin-2-yl)propanehydrazide derivatives (8a-d)

To a solution of the ester derivatives **(7)** (0.01mol) in ethanol (10 mL), hydrazine hydrate (0.02 mol) has added. The reaction mixture was stirred at room temp., for 1h, then heated for 3 h. The separated acid hydrazide products were filtered and recrystallized from ethanol.

3-(3-Oxo-3,4-dihydroquinoxalin-2-yl)propanehydrazide (8a) [61]

3-(6-Bromo-3-oxo-3,4-dihydroquinoxalin-2-yl)propane hydrazide (8b)

Light brown powder; Yield: (67%); m.p.: >300°C; IR (KBr, cm^{-1})= 3429, 3203 (br-NH_2 & 2NH), 3018 (CH-arom), 2919, 2848 (CH-aliph), 1683, 1656 (2C=O), 1602(C=N); ^{1}H NMR (400 MHz, DMSO-d_6) δ/ppm 2.72 (t, J = 7.0 Hz, 2H, CH_2), 3.05 (t, J = 7.0 Hz, 2H, CH_2), 5.02 (s, 2H, NH_2 exchangeable by D_2O), 7.14 (s, 1H, Ar-H), 7.42 (d, J = 8.8 Hz, 1H, Ar-H), 7.91 (d, J = 8.4 Hz, 1H, Ar-H), 10.79, 11.06 (2s, 2H, NH exchangeable by D_2O); ^{13}C NMR (101 MHz, DMSO) δ/ppm 29.02, 32.39 ($2CH_2$), 116.07, 122.39, 127.84, 129.00, 136.92, 147.97, 150.35 (C=N), 160.50, 180.33 (2C=O); MS (EI, 70 eV): m/z (%)= 313 [M^{+2}] (20.45%), 311 [M$^+$] (10.82%), 278 (100%); Anal. Calc. for $C_{11}H_{11}BrN_4O_2$ (311.14): C, 42.46; H, 3.56; N, 18.01; Found: C, 42.74; H, 3.69; N, 18.39.

3-(6-Chloro-3-oxo-3,4-dihydroquinoxalin-2-yl)propane hydrazide (8c) [58]

Light violet powder; Yield: (98) %; m.p.: >300°C; IR (KBr, cm^{-1})= 3286, 3160 (NH_2 & 2NH), 3065 (CH-arom), 2931, 2850 (CH-aliph), 1660 (br-2C=O), 1607 (C=N); ^{1}H NMR (400 MHz, DMSO-d_6): δ/ppm 2.68 (t, J = 6.6 Hz, 2H, CH_2), 3.02 (t, J = 7.6 Hz, 2H, CH_2), 4.24 (s, 2H, NH exchangeable by D_2O), 7.31(d, 1H, Ar-H), 7.32 (s, 1H, Ar-H), 7.71 (d, J = 8.0 Hz, 1H, Ar-H), 9.04, 10.86 (2s, 2H, NH exchangeable by D_2O); MS (EI, 70 eV): m/z (%)= 268 [M^{+2}] (5.81%), 266 [M·$^+$] (15.97%), 235 (1005%); Anal. Calc. for $C_{11}H_{11}ClN_4O_2$ (266.69): C, 49.54; H, 4.16; N, 21.01; Found: C, 49.36; H, 4.33; N, 20.84.

3-(7-Benzoyl-3-oxo-3,4-dihydroquinoxalin-2-yl)propane hydrazide (8d)

Yellow powder; Yield: (72) %; m.p.: 200-202°C; IR (KBr, cm^{-1})= 3315, 3239, 3201(NH_2 & 2NH), 3055 (CH-arom), 2912,2860 (CH-aliph), 1673, 1665 (br C=O), 1614 (C=N); ^{1}H NMR (400 MHz, DMSO-d_6): δ/ppm 2.45 (t, J = 7.6 Hz, 2H, CH_2), 3.03 (t, J = 7.0 Hz, 2H, CH_2), 4.18 (s, 2H, NH exchangeable by D_2O), 7.25 (d, J = 7.2 Hz, 1H, Ar-H), 7.31 (t, J = 6.8 Hz, 2H, Ar-H), 7.44 (d, J = 8.4 Hz, 1H, Ar-H), 7.52 (d, J = 7.2 Hz, 1H, Ar-H), 7.58 (d, J = 7.6 Hz, 2H, Ar-H), 7.78 (dd, J = 8.8, 2.0 Hz, 1H, Ar-H), 8.94, 9.01 (2s, 2H, NH exchangeable by D_2O); ^{13}C NMR (101 MHz, DMSO) δ 25.95, 29.97 ($2CH_2$), 118.13, 119.34, 121.22, 122.68, 124.44, 127.01, 129.44, 129.68, 130.23, 133.77, 134.13, 138.33, 155.35 (C=N), 160.61, 179.18, 194.28 (3C=O); MS (EI, 70 eV): m/z (%)= 336 [M·$^+$] (24.25%), 135 (100%); Anal. Calc. for $C_{18}H_{16}N_4O_3$ (336.35): C, 64.28; H, 4.79; N, 16.66; Found: C, 64.03; H, 4.54; N, 16.95.

***N'*-(3-(3-Oxo-3,4-dihydroquinoxalin-2yl)propanoyl) benzohydrazides (9a, b)**

A solution of quinoxaline derivative **8a** (2.32 g, 0.01 mol) and acid chlorides (0.01 mol) in DMF (10 mL) has heated under reflux for 4 h, the reaction mixture was cooled, and the product was collected and crystallized from ethanol.

***N'*-(3-(3-Oxo-3,4-dihydroquinoxalin-2yl)propanoyl) benzohydrazide (9a)**

Off white powder; Yield: (46%); m.p.: 190-192 °C; IR (KBr, cm^{-1})= 3441- 3201 (br-NH), 3011 (CH-arom), 2973, 2900, 2850 (CH-aliph), 1686, 1664 (C=O), 1601 (C=N); ^{1}H NMR (400 MHz, DMSO-d_6): δ/ppm 2.75 (t, J = 7.6 Hz, 2H, CH_2), 3.10 (t, J = 7.6 Hz, 2H, CH_2), 7.32 (t, J = 6.2 Hz, 1H, Ar-H), 7.51 (t, J = 6.8 Hz, 2H, Ar-H), 7.55 (d, J = 8.0 Hz, 1H, Ar-H), 7.60 (t, J = 7.6 Hz, 1H, Ar-H), 7.89 (t, J = 7.6 Hz, 1H, Ar-H), 7.95 (d, J = 7.2 Hz, 3H, Ar-H), 9.42, 10.11, 10.78 (3s, 3H, NH exchangeable by D_2O); MS (EI, 70 eV): m/z (%)= 337 [M^{+1}] (4.15%), 336 [M·$^+$] (9.08%), 124 (100%); Anal. Calc. for $C_{18}H_{16}N_4O_3$ (336.35): C, 64.28; H, 4.79; N, 16.66; Found: C, 64.18; H, 4.75; N, 16.59.

4-Fluoro-N'-(3-(3-oxo-3,4-dihydroquinoxalin-2-yl)propanoyl)benzohydrazide (9b)

Light green powder; Yield: (66%); m.p.: >300 °C; IR (KBr, cm^{-1})= 3443, 3321, 3222 (3NH), 3014 (CH-arom), 2903, 2851 (CH-aliph.), 1667 (br-C=O), 1604 (C=N); ^{1}H NMR (400 MHz, DMSO-d_6): δ/ppm 2.71 (t, J = 7.6 Hz, 2H, CH_2), 3.07 (t, J = 7.6 Hz, 2H, CH_2), 7.29 (t, J = 7.4 Hz, 2H, Ar-H), 7.33 (d, J = 8.8 Hz, 2H, Ar-H), 7.48 (d, J = 7.6 Hz, 1H, Ar-H), 7.73 (d, J = 7.6 Hz, 1H, Ar-H), 7.93 (d, J = 8.8 Hz, 2H, Ar-H), 9.98, 10.33, 12.31 (3s, 3H, NH exchangeable by D_2O); ^{13}C NMR (100 MHz, DMSO-d_6) δ/ppm 28.48, 29.78 ($2CH_2$), 115.65, 115.76, 115.98, 123.47, 128.59, 129.46, 129.88, 130.51, 130.60, 131.95, 132.17, 155.01 (C=N), 160.91 (C=O of Quinoxaline), 163.32 (C=O of benzoyl), 164.86 (C-F), 171.43 (C=O of propionyl derivatives); MS (EI, 70 eV): m/z (%)= 354 [M·$^+$] (21.23%), 43 (100); Anal. Calc. for $C_{18}H_{15}$ FN_4O_3 (354.34): C, 61.01; H, 4.27; N, 15.81; Found: C, 61.00; H, 4.37; N, 15.91.

***N'*-(Arylidene)-3-(3-oxo-3,4-dihydroquinoxalin-2-yl)propanehydrazide (10a, b)**

A mixture of quinoxaline derivative **8a** (2.32 g, 0.01 mol) and aromatic aldehydes (0.01 mol) in ethanol (20 mL) containing few drops of DMF has heated under reflux for 3 h. The reaction mixture cooled, and the product was collected and recrystallized from benzene.

***N'*-(4-Methylbenzylidene)-3-(3-oxo-3,4-dihydroquinoxalin-2-yl)propane-hydrazide (10a)**

Brick red powder; Yield: (56%); m.p.: 240-242°C; IR (KBr, cm^{-1})= 3443, 3206 (2NH), 3058 (CH-arom), 2906, 2852 (CH-aliph), 1660 (C=O), 1609 (C=N); ^{1}H NMR (400 MHz, DMSO-d_6) δ/ppm 2.32 (s, 3H, CH_3), 2.78 (t, J = 7.8 Hz, 2H, CH_2), 3.12 (t, J = 7.4 Hz, 2H, CH_2), 7.22 (d, J = 7.2 Hz, 1H, Ar-H), 7.26 (d, J = 6.0 Hz, 1H, Ar-H), 7.30 (d, J = 8.8 Hz, 1H, Ar-H), 7.47 (d, J = 7.2 Hz, 1H, Ar-H), 7.57

(t, J = 6.8 Hz, 2H, Ar-H), 7.69 (d, J = 7.2 Hz, 1H, Ar-H), 7.99 (d, 1H, Ar-H), 8.14 (s, 1H, CH-methine), 11.20, 11.43 (2s, 2H, NH exchangeable by D_2O); ^{13}C NMR (100 MHz, DMSO-d_6) δ/ppm 21.43 (CH_3), 28.82, 31.20 ($2CH_2$), 115.63, 115.69, 123.42, 123.49, 127.05, 127.33, 128.48, 129.80, 131.94, 132.07, 132.14, 142.98, 155.02, 162.73 (C=N), 168.36, 173.93 (2C=O); MS (EI, 70 eV): m/z (%)= 334 [M^+] (12.67%), 303 (100%); Anal. Calc. for $C_{19}H_{18}N_4O_2$ (334.38): C, 68.25; H, 5.43; N, 16.76; Found: C, 68.14; H, 5.42; N, 16.66.

_N'_-(4-(Dimethylamino)benzylidene)-3-(3-oxo-3,4-dihydro quinoxalin-2-yl)propanehydrazide (10b)

Deep yellow powder; Yield: (79%); m.p.: 270-272°C; IR (KBr, cm^{-1})= 3201 (br-NH), 3054 (CH-arom), 2968, 2896, 2850 (CH-aliph), 1663 (2C=O), 1604 (C=N); ^1H NMR (400 MHz, DMSO-d_6): δ/ppm 2.74 (t, J = 7.4 Hz, 2H, CH_2), 2.96 (s, 3H, -N-CH_3), 3.00 (s, 3H, -N-CH_3), 3.11 (t, J = 7.2 Hz, 2H, CH_2), 6.73 (d, J = 8.8 Hz, 1H, Ar-H), 6.78 (d, J = 8.8 Hz, 2H, Ar-H), 7.28 (t, J = 7.8 Hz, 1H, Ar-H), 7.31 (t, J = 6.4 Hz, 1H, Ar-H), 7.48 (d, J = 8.8 Hz, 1H, Ar-H), 7.66 (d, J = 8.8 Hz, 1H, Ar-H), 7.70 (d, J = 8.0 Hz, 1H, Ar-H), 8.51 (s, 1H, CH-methine), 10.98, 12.31 (2s, 2H, NH exchangeable by D_2O); MS (EI, 70 eV): m/z (%)= 363 [M^+] (8.63%), 43 (100%); Anal. Calc. for $C_{20}H_{21}N_5O_2$ (363.42): C, 66.10; H, 5.82; N, 19.27; Found: C, 66.18; H, 5.94; N, 19.17.

3-(3-Oxo-3,4-dihydroquinoxalin-2-yl)-_N'_-(1-arylethylidene) propanehydrazide (11a, b)

A mixture of quinoxaline derivative **8a** (2.32 g, 0.01 mol), and acetophenone derivatives (0.01 mol) in ethanol (20 mL) containing few drops of DMF was heated under reflux for 8h. The reaction mixture was cooled, and the solid product was collected and re-crystallized from ethanol.

3-(3-Oxo-3,4-dihydroquinoxalin-2-yl)-_N'_-(1-phenylethylidene) propanehydr-azide (11a)

White powder; Yield: (68%); m.p.: 250-252°C. IR (KBr, cm^{-1})= 3185, 3103 (2NH), 3063 (CH-arom), 2971, 2902, 2849 (CH-aliph.), 1683, 1662 (2C=O), 1605 (C=N); ^1H NMR (400 MHz, DMSO-d_6) δ/ppm 2.25 (s, 3H, CH_3), 2.74 (t, 2H, CH_2), 3.11 (t, J = 7.0 Hz, 2H, CH_2), 7.26 (t, J = 6.8 Hz, 1H, Ar-H), 7.38 (d, 1H, Ar-H), 7.46 (t, J = 6.4 Hz, 3H, Ar-H), 7.68 (t, J = 8.8 Hz, 1H, Ar-H), 7.77 (d, J = 6.8 Hz, 1H, Ar-H), 7.91 (d, J = 8.0 Hz, 1H, Ar-H), 7.93 (d, J = 8.8 Hz, 1H, Ar-H), 10.44, 12.41 (2s, 2H, NH exchangeable by D_2O); MS (EI, 70 eV): m/z (%)= 334 [M+·] (10.95%), 90 (100%); Anal. Calc. for $C_{19}H_{18}N_4O_2$ (334.38): C, 68.25; H, 5.43; N, 16.76; Found: C, 68.13; H, 5.55; N, 16.66.

_N'_-(1-(4-Chlorophenyl)ethylidene)-3-(3-oxo-3,4-dihydro quinoxalin-2-yl)propanehydrazide (11b)

Yellow powder; Yield: (83%); m.p.: 240-242°C; IR (KBr, cm^{-1})= 3244, 3184 (2NH), 3087 (CH-arom), 2966, 2896, 2847 (CH-aliph), 1668 (br-2C=O), 1624 (C=N); ^1H NMR (400 MHz, DMSO-d_6): δ/ppm 2.27 (s, 3H, CH_3), 2.75 (t, 2H, CH_2), 3.10 (t, 2H, CH_2), 7.25 (d, J = 8.4 Hz, 1H, Ar-H), 7.30 (d, J = 7.6 Hz, 1H, Ar-H), 7.47 (t, J = 7.6 Hz, 2H, Ar-H), 7.67 (d, J = 8.0 Hz, 1H, Ar-H), 7.80 (d, J = 8.4 Hz, 2H, Ar-H), 7.97 (d, J = 7.2 Hz, 1H, Ar-H), 10.51, 12.20 (2s, 2H, NH exchangeable by D_2O); ^{13}C NMR (100 MHz, DMSO-d_6) δ/ppm 19.00 (CH_3), 29.26, 31.26 ($2CH_2$), 115.58, 123.43, 128.10, 128.41, 128.50, 128.77, 129.22, 129.77, 130.52, 131.92, 133.98, 137.52, 146.13, 155.06 (2C=N), 162.73, 174.90 (2C=O); MS (EI, 70 eV): m/z (%)= 370 [M^{+2}] (2.67%), 368 [M^+] (6.25 %), 350 (100%); Anal. Calc. for $C_{19}H_{17}ClN_4O_2$ (368.82): C, 61.88; H, 4.65; N, 15.19; Found: C, 61.58; H, 4.42; N, 15.03.

2.2. Anticancer activity

2.2.1. Cytotoxicity screening

The cells were cultured in RPMI-1640 medium with 10% fetal bovine serum. Antibiotics were added 100 units/mL penicillin and 100 µg/mL streptomycin at 37°C in a 5% CO_2 incubator. The cells were seeded in a 96-well plate at a density of 1.0×10^4 cells/well at 37°C for 48 h under 5% CO_2. After incubation, the cells were treated with different concentrations of compounds and incubated for 24 h (three independent experiments were performed for each conc. of the tested compounds). Discard the medium. Fix with 10% trichloroacetic acid (TCA) 150 μL/well for 1 h at 4 °C. Wash by water 3 times (TCA reduces SRB protein binding). Wells will be stained by SRB 70 μL/well for 10 min at room temperature with 0.4%. 70 μL/well [keep in dark place]. Wash with acetic acid 1% to remove unbound dye (end-point: colorless drainage). The plates will be air-dried for 24 h. The dye will be solubilized with 50 μL/well of 10 mMtris base (PH 7.4) for 5 min on a shaker at 1600 rpm. The optical density (OD) of each well will be measured at 570 nm with an ELISA microplate reader (EXL 800 USA). The relative cell viability in percentage was calculated as (A570 of treated samples/A570 of the untreated sample) X 100, and The IC_{50} values will be calculated using sigmoidal concentration response curve fitting models (Sigmaplot software) [62–64].

2.2.2. Caspase-3 activation

Quantikine-Human active Caspase-3 Immunoassay (R&D Systems, Inc. Minneapolis, USA) was used to detect caspase-3 level; this was performed on MCF-7 cells according to the manufacturer protocol by Adding 100 μL of the standard diluent Buffer to the zero standard wells. Then add 100 μL of standards and controls or diluted samples to the appropriate microtiter wells. Cover and incubate for 2 h at room temperature. Add 100 µL of Caspase-3 (Active) Detection Antibody solution into each well except the blank. Incubate for 1 h (twice experiments were performed for each concentration), then add 100 μL Anti-Rabbit IgG HRP Working Solution to each well except the chromogen blank and incubate for 30 min. Add 100 μL of Stabilized Chromogen to each well. Finally, read the absorbance of each well at 450 nm [65].

2.2.3. Study on mitochondrial proteins BAX and Bcl-2

Cells were obtained from American Type Culture Collection. Cells were grown in RPMI 1640 containing 10% fetal bovine serum at 37°C, stimulated with the compounds to be tested for BAX or Bcl-2 and lysed with Cell Extraction Buffer. This lysate was diluted in Standard Diluent Buffer over the assay range and measured for human active BAX or Bcl-2 content. (cells are Plated in a density of 1.2-1.8 × 10,000 cells/well in a volume of 100 µL complete growth medium + 100 uL of the tested compound per well in a 96-well plate for 24 h before measured for human active BAX or Bcl-2.

2.2.4. Cell cycle analysis

MCF-7 cells were seeded in a 6-well plate at 1 × 10^5 cells per well and incubated for 24 h. The cells were treated with vehicle (0.1% DMSO) or 10 µM of the selected compounds for 24 h (each experiment was repeated twice). Cells were harvested and fixed with ice-cold 70% ethanol at 4ºC for 12 h. Ethanol was removed, and the cells were washed with cold PBS. Then cells were incubated in 0.5 mL of PBS containing 1 mg/mL Ranse for 30 min at 37ºC. Then the cells were stained with propidium iodide in the dark for 30 min. The DNA contents were then measured by a flow cytometer [66].

2.2.5. Annexin-V assay

MCF-7 cells were seeded in a 6-well plate (1 × 10^5cells/well). After incubation for 24 h, the cells were treated with vehicle (0.1% DMSO) or 10 µM of the selected compound for 24h (each experiment were repeated twice). The cells were then harvested and washed with PBS, then stained with annexin V-FITC and PI in binding buffer (10 mM HEPES, 140 mM NaCl and 2.5 mM $CaCl_2$ at pH 7.4) for 15 min at room temperature in the dark. The samples were analyzed using the flow cytometer, as mentioned above [67].

2.2.6. EGFR assay

Inhibitory activity of most promising compounds **3a, 6, 7b** and **7d** on MCF-7 cells were performed against $EGFR^{wt}$ and $EGFR^{L858R-TK}$ using the same instructions from the manufacturer protocol and according to reported methods [35,64]. For $EGFR^{wt}$ inhibition assay was performed on MCF-7 cells using cloud clone SEA757Hu 96 Kit. The fraction of the EGFR was measured in the presence of the tested compounds using the equation: E (%) = E max/(1 + [I]/ID_{50}), E max is the activity in the absence of the inhibitor, [I] is the inhibitor concentration, and ID_{50} is the inhibitor concentration when E (%) = 0.5 E max. The dose–response curve was plotted. The values represent a mean of two independent experiments [68]. While Inhibitory activity against EGFR L858R-TK, performed using HTRF (homogeneous time-resolved fluorescence) assay method [69], using BioAssay Systems' EnzyChromTM Kinase Assay Kit. The specified kinase (EGFR L858R-TK) and its substrate were incubated with the tested compounds **3a, 6, 7b**, and **7d** and reference drug for 5 min in a buffer solution to start the enzymatic reaction, then ATP added to the reaction mixture. They were maintained for 30 min at room temperature. Stopping the reaction occurred by adding detection reagents containing EDTA for 1 h. then the IC50 values were determined by GraphPad Prism 5.0.

2.2.7. Molecular docking study

X-ray crystallographic structure of the EGFR co-crystallized with 4-anilinoquinazoline inhibitor (Erlotinib) as a ligand obtained from protein data bank (PDB ID:1M17) [70]. The docking process was performed according to the standard protocol described in our previous work [35,64,71], where all minimizations performed with MOE with MMFF94x force field and the partial charges were automatically calculated. Triangle Matcher placement method and London dG scoring function (strength of binding) selected in the docking process. The validation process by re-docking of the co-crystallized ligand (L) (Erlotinib) performed to generate the active site, and the co-crystalized (Erlotinib) exhibited energy score (S) = -17.84 kcal/mol, with RMSD of 1.10 °A with MMFF94x force field. The quinoxaline derivatives that docked were prepared by drawn in ChemDraw 14, exported to MOE, protonated 3D, minimized energy and render hydrogen was performed and finally saved as mdb file.

3. Results and Discussion

3.1. Chemistry

The synthetic strategies adopted for the synthesis of the target compounds are depicted in Scheme 1 to Scheme 3. Cyclo-condensation of 1,2-diaminobenzene derivatives **1** with dimethyl acetylene dicarboxylate in ethanol at room temperature furnished methyl 2-(3-oxo-3,4dihydroquinoxalin-2(1*H*)-ylidene)acetate derivatives **(2a-c)** [72]. The structure of compound **2b** proved based on elemental and spectral data. The IR spectrum showed bands at 3218, 1693, and 1652 cm^{-1} for NH, C=O ester, and C=O amidic (Scheme 1). The ^1H NMR spectrum of **2b** in DMSO-d_6 showed two singlet signals at δ 3.67 and 5.54 ppm corresponding for methoxy ester and vinylic protons, besides two singlet signals at δ 10.99, 11.77 ppm for 2NH exchangeable protons with D_2O. The subsequent reaction of methyl ester derivatives **2a-c** with hydrazine hydrate in ethanol under reflux condition afforded the corresponding acetohydrazide quinoxaline derivatives **3a-c**. IR spectrum of **3c** showed stretching absorption bands at 3288, 3200, and 1674 cm^{-1} were attributed to NH, NH_2, and carbonyl functional groups. Its ^1H NMR spectrum (DMSO-d_6) revealed a signal at δ 4.28 ppm related to an amino group that exchangeable by deuterium. Furthermore, a signal at δ 5.56 ppm for CH-vinylic, multiples aromatic protons between δ 7.22 to 7.59 ppm and three singlet signals at δ 6.92, 9.13, 11.58 ppm for three NH which exchangeable by D_2O.

Besides, condensation of 1,2-diaminobenzene or its chloro/bromo derivatives with α-ketoglutaric acid in acetic acid yielded 3-(3-oxo-3,4-dihydroquinoxalin-2-yl)propionic acid derivatives **(4a-c)** in good yields, where the chloro or bromo substituent was in the 6-position. Similarly, 4-benzoyl-1,2-phenylinediamine afforded 3-(7-benzoyl-3-hydroxyquinoxalin -2-yl)propanoic acid **(4d)** not 6-benzoyl derivative that formed by a resonance effect of benzoyl moiety (electron-withdrawing group) where (-R) of the benzoyl moiety caused deactivation of the *p*-amino group, and the *m*-amino group initiated the reaction (Scheme 2). The structure elucidation of the prepared compounds based on spectral data and elemental analyses. The IR spectrum of compound **4b** revealed a band around 3413 cm^{-1} assignable to the hydroxyl group, in addition to presence of bands at 3150, 1689, 1670, and 1603 cm^{-1} corresponding for NH, two carbonyl (C=O), and C=N, respectively. Also, the ^1H NMR spectrum of compound **4b** showed two triplets at δ 2.68 and 2.98 ppm for two CH_2 groups and two singlet signals for NH and OH protons, which appeared at δ 12.36, 12.42 ppm (D_2O exchangeable), confirming the formation of the compound. Its ^{13}C NMR spectrum displayed two signals at δ 28.12, and 29.90 ppm for $2CH_2$, besides two signals observed at δ 161.45 and 174.24 ppm due to two carbonyl groups. Its mass spectrum displayed a molecular ion peak at m/z = 297, corresponding to a molecular formula $C_{11}H_9BrN_2O_3$ with a base peak at m/z = 252. Moreover, the reaction of 3-(3-oxo-3,4-dihydroquinoxalin-2-yl)propanoic acid **(4a)** with thionyl chloride in dry benzene for obtaining the acid chloride **(5)** was unsuccessful. Therefore 3,4-dihydro-2*H*-pyrano[2,3-*b*]quinoxalin-2-one **(6)** was obtained as the reaction product on the basis of its elemental analysis and spectral data. The IR revealed an absorption band at 1688 cm^{-1} corresponding to the (C=O) group. Its ^1H NMR spectrum showed two triplet signals at δ 2.70 and 2.99 ppm corresponding for two CH_2 groups in addition to aromatic protons in the region δ 7.26-7.67 ppm. Its ^{13}C NMR exhibited two signals at δ 28.08 and 30.03 ppm for the two methylene groups and δ 174.31 ppm for the carbonyl group.

Esterification of quinoxaline carboxylic acid derivatives **4** using the traditional method in the presence of sulfuric acid afforded the corresponding methyl or ethyl ester derivatives **(7a-g)**, as shown in scheme 3. The assignment of the structures **7a-g** based on analytical and spectroscopic data. Thus, the IR spectrum of quinoxaline derivative **7c** displayed absorption bands at 3442, 1725, and 1662 cm^{-1} assignable to NH and two C=O groups for the ester and amidic NH groups, respectively. Its ^1H NMR spectrum showed two singlet signals at δ 1.07 and 4.11 ppm for the ethyl group that appears as a triplet and quartet, and two triplet signals displayed at δ 2.78 and 3.05 ppm due to the two methylene groups. In contrast, the aromatic protons were observed between δ 7.27-7.68 ppm. The exchangeable singlet signal for the NH group appeared at δ 12.41 ppm.

Hydrazinolysis for the ester derivatives **7a-g** with hydrazine hydrate in ethanol afforded the hydrazide derivatives **8a-d**. The chemical structures of compounds **8a-d** are confirmed by elemental analysis and spectral data. The IR spectrum of compound **8b** as a representative example showed the lake of ester band and new absorption bands appear at 3429, 3203 cm^{-1} for NH_2, NH groups, in addition to two bands at 1683, 1656 cm^{-1} for two carbonyl groups. Its ^1H NMR spectrum exhibited two triplet signals at δ 2.72 and 3.05 ppm for $2CH_2$ protons. The NH_2 and two NH bands were observed at δ 5.02, 10.79, and 11.06 ppm, respectively. The mass spectrum of **8b** revealed a molecular ion peak at m/z=311 corresponding to a molecular formula $C_{11}H_{11}BrN_4O_2$ with a base peak at m/z= 278.

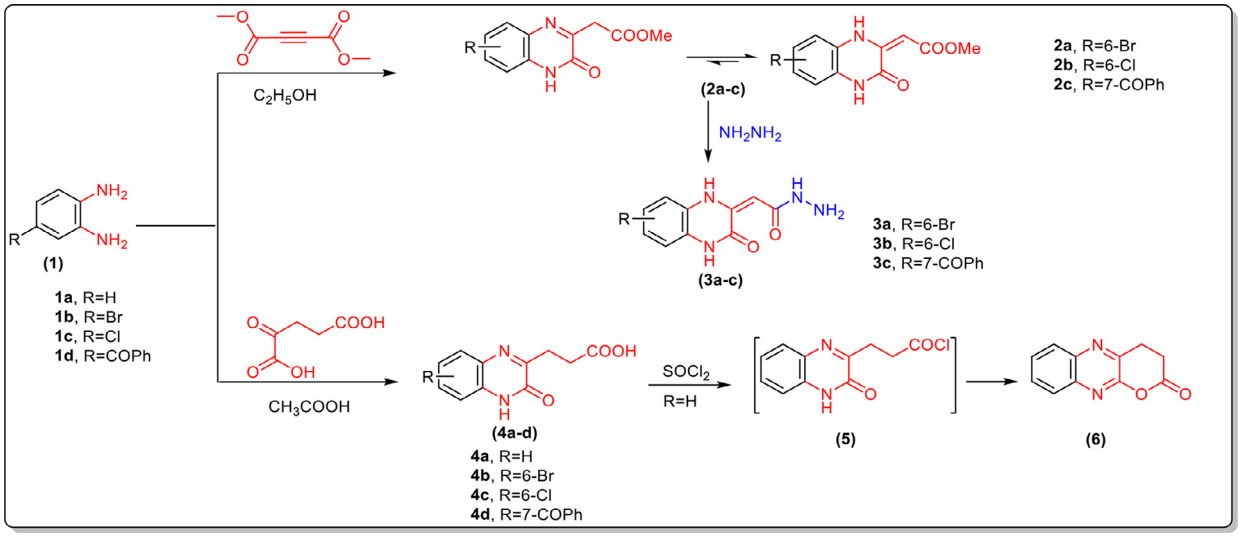

Scheme 1. The reaction of 1,2-diaminobenzene derivatives with dimethyl acetylene-dicarboxylate and α-ketoglutaric acid for synthetized quinoxaline derivatives.

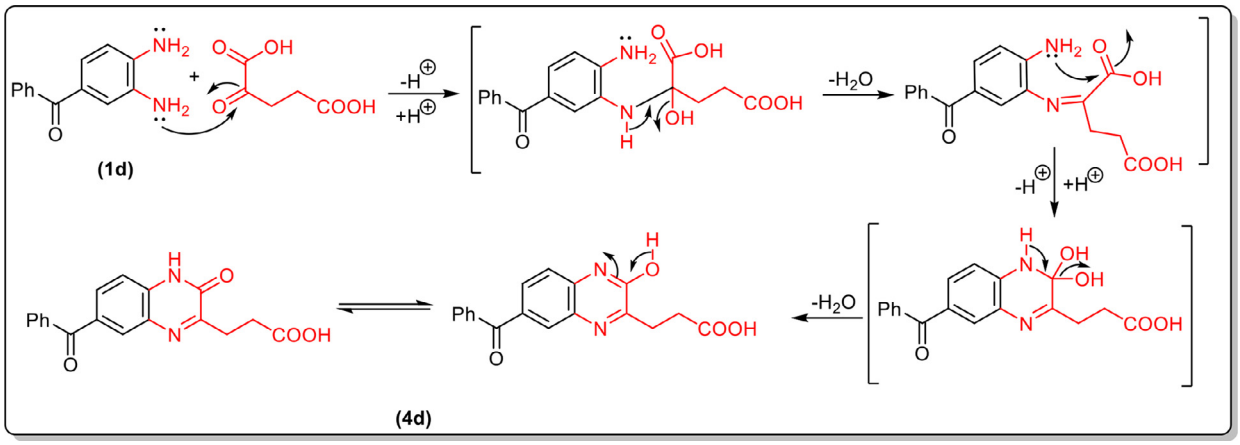

Scheme 2. Suggested mechanism illustrating the formation of benzoyl quinoxaline derivative **4d**.

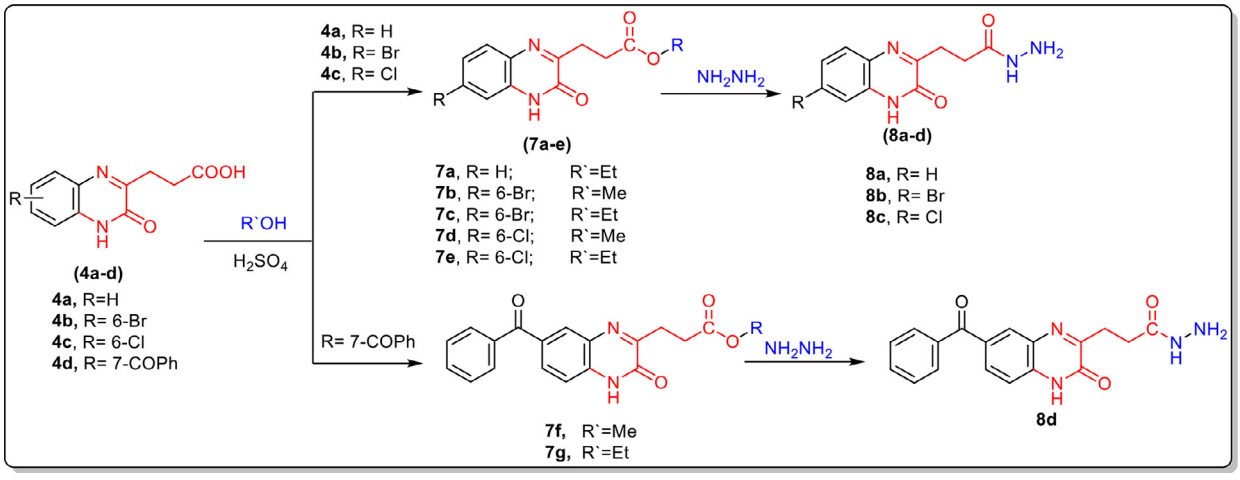

Scheme 3. Quinoxaline compounds with ester and hydrazide moieties.

Furthermore, different hydrazide and hydrazone derivatives **9-11** synthesized, starting from quinoxaline derivative **8a**. The reaction of compound **8a** with acid chloride derivatives furnished the corresponding benzoyl hydrazide derivatives **9a, b**. Analytical and spectral data confirmed the structure of the prepared compounds in scheme 4. The IR spectrum of compound **9b** revealed an absorption band at 3443, 3321, 3222, and 1667 cm^{-1} due to three NH as well as one carbonyl groups, while the ^1H NMR spectrum of the same compound in DMSO-d_6 showed three singlet signals at δ 9.98, 10.33, 12.31 ppm for 3NH protons which exchangeable with deuterated water, besides eight aromatic protons at δ 7.29-

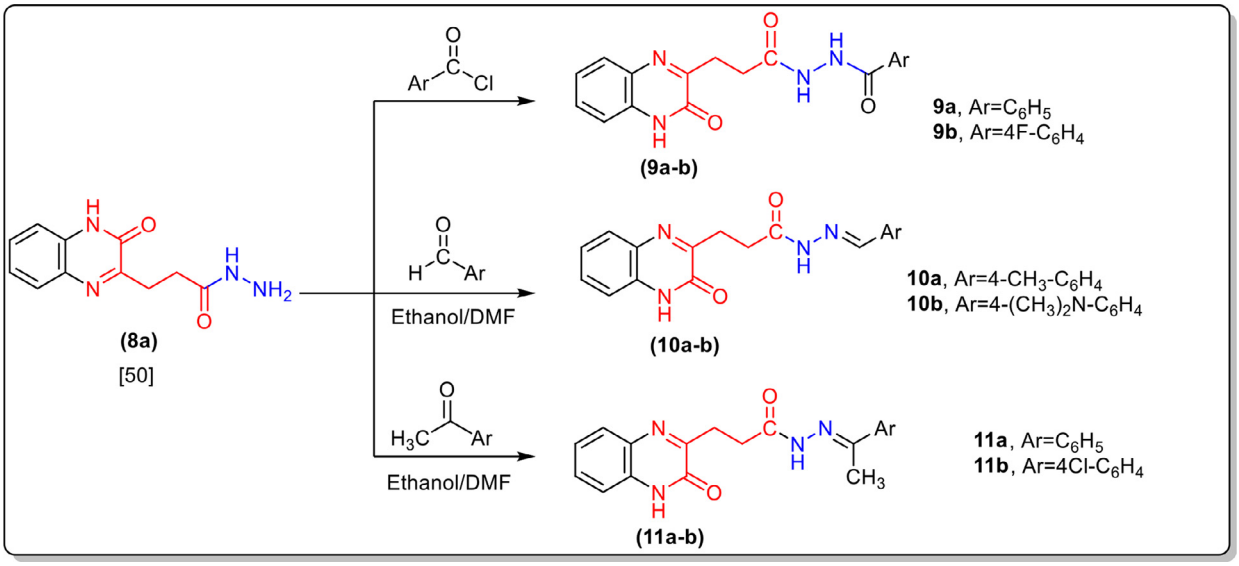

Scheme 4. The reaction of **8a** with benzoyl chloride, benzaldehyde, and acetophenones derivatives.

7.93 ppm. The ^{13}C NMR for compound **9b** exhibited two signals at δ 28.48 and 29.78 ppm for the two methylene groups and δ 155.01 (C=N), 160.91 carbonyl of quinoxaline, δ 163.32 ppm for carbonyl group attached to the phenyl ring δ 164.86 (C-F), and finally, δ 171.43 ppm for the carbonyl groups in the open chain. Also, condensation of quinoxaline derivative **8a** with aromatic aldehyde and acetophenone derivatives furnished the corresponding hydrazone derivatives **10a, b** and **11a, b**. The structure of the synthesized compounds agreed with analytical and spectral data. The ^{1}H NMR spectrum of **10a** in DMSO-d_6 showed characteristic singlet signal at δ 8.14 ppm for CH=N protons and two singlet signals at δ 11.20, 11.43 ppm for 2NH protons, which are all exchangeable with D_2O. Its ^{13}C NMR spectrum displayed a signal at δ 21.43 ppm for the CH_3 group and two signals at δ 28.82, and 31.20 ppm for $2CH_2$ groups of propane as well as two singlet signals observed at δ 168.36, 173.93 ppm due to two carbonyl groups. While the ^{1}H NMR spectrum of compound **11b** in DMSO-d_6 showed a singlet signal at δ 2.27 ppm due to CH_3 protons and two singlet signals at δ 10.51, 12.20 ppm for 2NH protons (exchangeable with D_2O), in addition to the eight aromatic protons ranging from δ 7.25 to 7.97 ppm. Its ^{13}C NMR spectrum of compound **11b** displayed a signal at δ 19.00 ppm for the CH_3 group and two signals at δ 29.26, and 31.26 ppm for $2CH_2$, besides two signals were observed at δ 162.73 and 174.90 ppm due to two carbonyl groups.

3.2. Pharmacological evaluation

3.2.1. Cytotoxicity screening

The cytotoxicity of all synthesized derivatives were assessed for three cancer cell lines as human hepatocellular carcinoma (HepG-2), human adenocarcinoma colorectal (HCT-116), and breast cancer (MCF-7) using SRB methods as reported [73,74]. Table 1 shows the results obtained. Compound **6** had the most potent effect against the tested three cell lines, with IC_{50} 10.05, 7.57 and 8.15 μM, respectively, compared with Doxorubicin as a reference standard.

It was observed that, on HepG-2 cancer cells, compounds **2c, 3a**, and **7b** showed IC_{50} values less than 20 µM (IC_{50} range: 15.58-18.57 µM). Besides, compounds **7b** and **7f** showed IC_{50} values less than or nearly equal 15 µM on HCT-116 cancer cells (IC_{50} nearly 13 µM). Compound **3b** also showed IC_{50} values below or nearly equal 15 µM on MCF-7 cancer cells (IC_{50} 13.65 µM). Compounds **3a, 7b,** and **7c** showed a range of IC_{50} less than 20 µM on MCF-7 cancer cell line, their IC_{50} range (16.86-18.52 µM). On the other hand, the most active compound on these cancer cells was compound **6**, and its IC_{50} values were less than (10 µM). Those positive findings inspired us to our new compounds' mechanistic studies. The cytotoxic activity has also been studied on healthy, non-cancer cells (WI-38 cells) (known as the diploid human cell line consisting of fibroblasts originating from the lung tissue of a 3-month aborted female fetus) as described in (Table 2). The tested derivatives revealed that the most promising compounds showed IC_{50} > 140 μM on human healthy, non-cancer cell lines (WI-38 cells), especially compounds **2c, 3a, 6**, and **7b** displayed IC_{50} values of less than 20 μM on HepG-2. Also, compound **6** exhibited anti-proliferative activity against HCT-116 was higher than that of the Doxorubicin. Furthermore, **3b** and **6** derivatives displayed IC_{50} values less than 15μM on MCF-7 cells.

Finally, the effect of the promising new derivatives on non-cancer cells revealed that the synthesized compounds had higher cytotoxic values IC_{50} = 142.21 μM. Such optimistic derivatives were selected for further study because of their potential as active anticancer agents **3a, 3b, 6, 7b, 7c, 7d**, and **7f**.

3.2.2. Structure-activity relationship (SAR)

We aimed to analyze the SAR for the newly synthesized quinoxaline derivatives as possible cancer agents from all previous results. The effect of substitution on the antitumor activities of the target compounds at various locations has been investigated. We synthesized two acrylate or propanoate pieces of the quinoxaline derivatives. Firstly, methyl acrylate quinoxaline showed moderate antitumor activity, and chloride derivative observed good activity against three antitumor cell lines than bromide and benzoyl. Further, the benzoyl derivatives exhibited the most potent of them against HepG-2 compared to ester and hydrazide derivates of acrylate quinoxaline with IC_{50} (15.85). Moreover, the activity of both bromide and chloride give abroad anti-proliferative activity to all tested cell lines in this study HepG-2, HCT- 116, and MCF-7 (18.57, 28.44, 16.86) and (22.75, 18.04, 13.65) for bromo and chloro derivatives respectively.

Benzoyl derivatives **3c** unexpected acetohydrazide displayed low cytotoxic activity (compared to methyl acrylate derivative **2c**). It was noted that ring closure as in compound **6**, with a hydrophobic moiety such as pyrano[2,3-b]quinoxalin-2-one, exhibited high inhibitory effect against all tested cells with IC_{50} less

Table 1
Cytotoxic activities IC_{50} (μM) of the synthesized compounds **2-11** and Doxorubicin against (HepG-2, HCT-116, MCF-7 and WI-38) cell lines.

Compd. No.	IC_{50} [a] (μM ± S. E)			
	HepG-2	HCT- 116	MCF-7	WI-38
2a	53.01± 0.86	47.15 ± 0.66	59.16 ± 1.05	284.23± 4.25
2b	32.18 ± 0.33	36.51 ± 0.88	29.88 ± 0.74	258.26± 2.58
2c	15.85 ± 0.28	51.34 ± 0.23	27.76 ± 0.89	274.41± 4.29
3a	18.57 ± 0.11	28.44 ± 0.44	16.86 ± 0.55	227.35± 2.96
3b	22.75 ± 0.22	18.04 ± 0.33	13.65 ± 0.46	335.03± 3.25
3c	50.41 ± 0.98	44.95 ± 0.55	100.67 ± 1.45	194.68± 3.47
4a	277.38 ± 5.12	245.32 ± 3.55	295.91 ± 2.53	ND
4b	66.58 ± 0.89	43.92 ± 1.09	44.0 ± 0.94	253.91± 1.32
4c	81.21 ± 1.54	28.18 ± 0.52	33.99 ± 0.67	258.14± 1.89
4d	97.48 ± 1.58	116.28 ± 1.89	94.86 ± 2.98	183.45± 1.24
6	10.05 ± 0.25	7.57 ± 0.15	8.15 ± 0.18	154.36±2.87
7a	97.19 ± 2.11	108.05 ± 2.36	86.13 ± 0.96	ND
7b	15.58 ± 0.25	13.75 ± 0.16	17.90 ± 0.73	142.21± 1.11
7c	37.24 ± 0.74	34.16 ± 0. 25	18.52 ± 1.28	162.93± 0. 98
7d	46.23 ± 1.02	31.57 ± 0.85	23.31 ± 0.65	242.08± 2.11
7e	26.93 ± 0.88	24.54 ± 0.96	25.39 ± 0.46	262.72± 2.13
7f	25.44 ± 0.95	13.61 ± 0.35	22.44 ± 1.03	226.49± 2.01
7g	41.47 ± 1.22	37.81 ± 0.45	37.04 ± 0.87	240.14± 3.02
8a	86.55 ± 1.98	82.45 ± 1.87	110.30 ± 0.98	ND
8b	164.52 ± 3.45	64.53 ± 0.75	64.46 ± 1.89	159.25± 1.25
8c	97.45 ± 0.95	99.17 ± 1.48	63.61 ± 0.47	234.54± 0.96
8d	125.31 ± 2.96	119.99 ± 0.48	79.14 ± 1.33	223.13± 2.51
9a	43.86 ± 1.08	37.14 ± 1.20	39.43 ± 2.80	ND
9b	44.77 ± 1.25	48.78 ± 1.46	63.38 ± 1.31	ND
10a	85.56 ± 2.63	70.29 ± 2.13	94.43 ± 1.55	ND
10b	33.74 ± 1.30	30.88 ± 1.10	39.20 ± 1.41	ND
11a	82.36 ± 2.17	56.13 ± 1.45	53.98 ± 1.81	ND
11b	53.94 ± 1.81	44.23 ± 1.61	85.07 ± 1.24	ND
Dox.	8.46 ± 0.12	8.24 ± 0.32	4.60 ± 0.02	ND

[a] Data represent the mean values of three independent determinations.ND: Not determined.

Table 2
Effect of compounds **3a, 3b, 6, 7b, 7c, 7d** and **7f** on the gene's expression of some apoptosis key markers at conc. 100 μL.

Cpd. No.	Caspase-3 (Folds) (ng/mL)	BAX Pg/mL	Bcl-2 Pg/mL	BAX/Bcl-2 ratio
3a	413.10 (8.63)	420.66	1.401	300
3b	320.20 (6.68)	279.25	2.551	109
6	512.17 (10.69)	389.56	1.687	231
7b	384.05 (8.02)	356.34	1.261	283
7c	353.70 (7.38)	302.50	1.803	168
7d	453.20 (9.46)	311.39	1.766	176
7f	276.60 (5.77)	286.5	2.574	111
MCF-7	47.88 (1.0)	38.74	5.027	7

than or nearly to doxorubicin drug. Next, we explored the effect of propanoic and propanoate substituents. In general, propionate ester typically offers wider and more active anti-proliferative derivatives than quinoxaline with propanoic acid or a propanoic hydrazide, in particular for MCF-7 cell lines. The methyl propionate of bromo quinoxaline derivatives **7b** exhibited good results against all tested cell lines with IC_{50} values ranging between 13.75 μM to 17.90 μM. Based on the IC_{50} values, the activity of quinoxaline propionate ester derivatives **7a-g** decreased in the following order **7b** > **7c** > **7f** > **7d** > **7e** > **7g**. However, the results are not as good as expected, compared to the ester or acid derivatives. We decided to investigate the substituents' effect by reacting hydrazine derivatives with certain acid chloride derivatives to produce hydrazide derivatives **9a, 9b**, hopefully, to obtain higher and broad anti-proliferative activity. The activity increased due to the presence of benzoyl more than 4-floro-benzoyl derivative. Furthermore, the presence of diethyl amine attached to benzaldehyde in position four in quinoxaline derivative **10b** caused an enhancement in the activity towards all tested cell lines but still less active than the Doxorubicin. For **10b** the IC_{50} values are for HepG-2, HCT-116 and MCF-7 (33.74, 30.88, 39.20 μM), respectively. Our research has been expanded to react with acetophenone derivatives to substitute benzylidene protons in **10a,b** with a methyl group of **11a,b**, but **10b** is still observing more activity the later designed derivatives.

3.2.3. Apoptosis detection studies

2.2.3.1. Effect on the active Caspase 3 level. Caspases (Cysteinyl Aspartate-specific Proteases) are a family of intracellular enzymes strictly controlling the apoptotic pathway and are implicated in the development of neurodegenerative disorders [75]. Caspases identified as initiating (e.g., Caspases 8, 9, and 10) and executing caspases (e.g., Caspases 3, 6, and 7). There are two pathways known to initiate apoptosis, first one by a particular protein which binds to the death receptor (death receptor pathway) and the other one by damaging DNA and therefore mitochondrial induction of the cell death program (mitochondrial pathway) [76].

In this work, some new derivatives that have shown promising anti-proliferative activity evaluated their ability to increase the caspase-3 enzyme level, the obtained data summarized in Table 2. Compounds **3a, 6, 7b, 7c** and **7d** showed the best Caspase 3 activity (353-512 ng/mL) on MCF-7 cells at concentration 100 μL for three and half hours compared to untreated MCF-7 cells and therefore increased in the level of caspase-3 by 8.6, 10.69, 8.02, 7.38 and 9.46 folds respectively. Compounds **3b, 7f** were found to be weak Caspase 3 activator (320.2 and 276.6 ng/mL) by 6.68 and 5.77 folds more than control. Compounds **3a, 3b**, and **7b** showed anticancer activity against the MCF-7 cell line with an IC_{50} value of less than 20 μM.

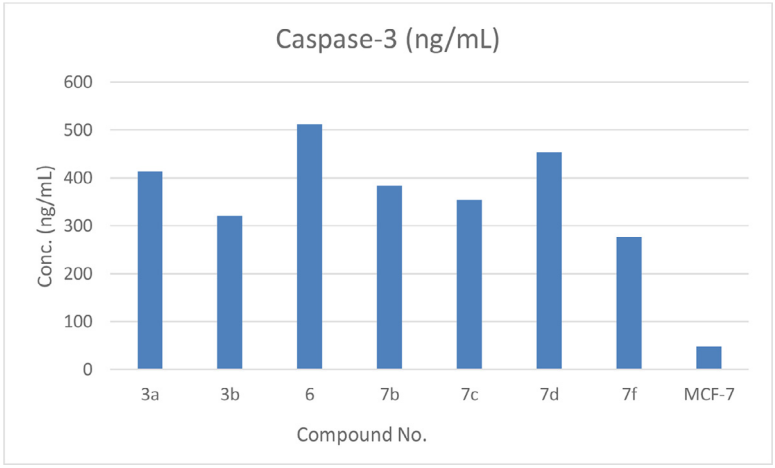

Fig. 3. A diagram illustrated the effect of quinoxaline derivatives **3a, 3b, 6, 7b, 7c, 7d** and **7f** regarding apoptotic induction of Caspase-3 on MCF-7 at concentration 100 µL for three and half hours.

Finally, pyrano[2,3-*b*]quinoxalin-2-one compound **6** showed IC_{50} value less than or equal to 10 µM on all the tested cell lines, as well as it has shown to be the best Caspase 3 activator in this series (10.69 folds) followed by quinoxaline derivatives **7d, 3a** and **7b** with (9.46, 8.63, and 8.02 folds) respectively. Fig. 3.

2.2.3.2. Effect on mitochondrial apoptosis pathway proteins BAX and Bcl-2. Bcl-2 and BAX are two distinct members of a family of genes involved in regulating cellular apoptosis known as the Bcl-2 family, which finely tunes the on/off mechanism of the apoptotic transition and is regarded as an important gatekeeper for the apoptotic reaction. If the Bcl-2 protein is functionally characterized as an apoptosis suppressing factor, then the BAX protein is considered as an apoptosis-promoting factor. The intracellular BAX/Bcl-2 ratio significantly impacts the cell's ability to respond to an apoptotic signal [77,78].

In this work, treatment of MCF-7 cells with the most promising quinoxaline derivatives **3a, 3b, 6, 7b, 7c, 7d**, and **7f** at 100 µL for 24 hs, resulted in substantial up-regulation of the expression level of the pro-apoptotic BAX protein by 7.2-10.6 folds compared to the untreated control. Besides, the tested derivatives showed a considerable concomitant decrease in the anti-apoptotic Bcl-2 protein expression level by approximately 1.95–3.99 folds compared to control (Table 2). The highest result was seen in compounds **3a, 6, 7b**, and **7d**, respectively, which increase the BAX level by (10.6, 10.9, 9.2 and 8.04 folds), besides the Bcl-2 level reduced by (3.6, 3.0, 3.9, and 2.85 folds) compared with the control, respectively. These findings showed that the BAX / Bcl-2 ratio 109-300 folds were substantially increased in comparison to control for all screened derivatives.

3.2.4. Cell cycle analysis

Compounds **3a, 6, 7b**, and **7d** were further investigated through cell cycle analysis, which was performed on MCF-7 cancer cells, upon treating them with 10 µM for 24 hs, of these compounds. The representative cell cycle distribution histogram of the stained DNA of the cancer cells is shown in Figs. 4, 5 and Table 3, when treated with the most promising derivatives.

The obtained results revealed the accumulation of MCF-7 cells after treating with compounds **3a, 6, 7b**, and **7d** at the G0/G1 phase with 46.3, 51.4, 49.4, and 39.4%, respectively, in comparison to the untreated cells 55.81 % (Table 3). However, compound **6** induced apoptosis at the S phase with 15.45%, while in Sub-G1 7.27% (Fig. 4, 5). Compound **7d** caused cell cycle arrest at the G2-M phase by 48%, while 17.25, 12.55 % for Sub-G1, and S phases. All the promising compounds exhibited an increased cell cycle arrest in both G2-M with percentage ranged between (26.25-48%) and Sub-G1 between (7.27 to 17.25 %) compared to untreated cell (14.21 and 2.16 %), respectively, especially compound **7d**.

Table 3
Results of cell cycle analysis in MCF-7 expressed by (%) cells in each phase when treated with compounds **3a, 6, 7b**, and **7d** by 10 µM for 24 h.

Compd. No.	Results			
	%G0-G1	%S	%G2-M	%Sub-G1
3a	46.33	16.14	37.53	13.39
6	51.64	15.45	32.91	7.27
7b	49.42	24.33	26.25	11.29
7d	39.45	12.55	48	17.25
MCF-7	55.81	29.98	14.21	2.16

Table 4
Percent of cell death induced by 10 µM for 24 h of **3a, 6, 7b**, and **7d** compounds on MCF-7 cells.

Cpd. No.	Total	Apoptosis %		Necrosis
		Early	Late	
3a	13.39	3.81	7.3	2.28
6	7.17	1.77	3.2	2.2
7b	11.29	2.84	5.84	2.61
7d	17.25	3.67	9.51	4.07
MCF-7	2.16	0.38	0.22	1.56

3.2.5. Apoptosis induction

For further evaluation of the cell death pathway induced with the tested compounds, Annexin V/propidium iodide (PI) double staining assay used to investigate and distinguish between necrotic cell death and apoptosis, induced **MCF-7** cell death when treated with the tested compounds **3a, 6, 7b** and **7d**, for 24 h with 10 µM from each tested compound. The obtained results that represented different percent of cell death are shown in Fig. 6 and Table 4. Compounds **3a, 7b,** and **7d** proved to induce apoptosis by

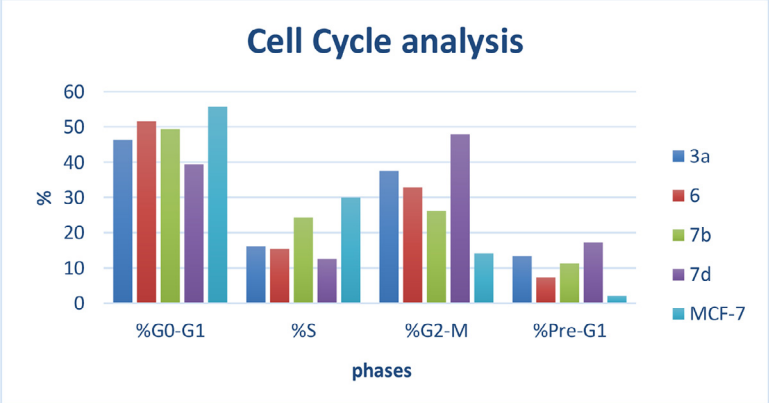

Fig. 4. Cell cycle analysis and apoptosis effect in MCF-7 cell line treated with compounds **3a, 6, 7b** and **7d** by 10 µM for 24 h.

Table 5
IC_{50} of the representative anticancer active compounds on EGFR wide and mutant (L858R-TK) in MCF7 cells.

Compd. No.	Enzyme inhibitory activity IC_{50}	
	$EGFR^{WT}$ (µM)	$EGFR^{L858R-TK}$ (nM)
3a	1.547	87.34
6	0.075	63.70
7b	0.957	75.42
7d	1.34	82.76
Erlotinib	0.0656	59.56

3.81, 1.77, 2.84, and 3.67 %, respectively, at the early stage of apoptosis. Also, from Fig. 6 and Table 4, we could conclude that the treatment of **MCF-7** cells increased total apoptosis percentage from 0.6% for **MCF-7** cells to 13.18, 11.11, 8.68, 4.97% when treated with compounds **7d, 3a, 7b, 6**, respectively.

3.2.6. EGFR inhibition assay

The Epidermal Growth Factor (EGFR) is considered a desirable and scientifically established target for cancer care drugs. The development and advancement of cancers such as cell proliferation, adhesion, migration, differentiation, and survival are important for various biological processes. Two separate mechanisms can cause EGFR dysregulation, one of which is high EGFR expression, and the other involves ligand over-expression and hence EGR signaling activity, provided normal or low receptor expression rates [79,80], and therefore the EGFR may cause dysregulation.

We have selected the most promising compounds for the MCF-7, **3a, 6, 7b**, and **7d** EGFR enzyme activity tests. The $EGFR^{WT}$ findings for MCF-7 cancer cells were identified as half the average inhibitory concentration of IC_{50} (μM) represented in (Table 5). All the compounds tested showed less than 2 μM of the $EGFR^{WT}$ inhibitory assay. The pyrano[2,3-*b*]quinoxalin-2-one derivatives (**6**) found to be the highest IC_{50} value relative to the Erlotinib reference level, followed by **7b, 7d**, and **3a** with IC_{50} values (0.075, 0.957, 1.34 and 1.547) μM, respectively.

Due to the importance of EGFR, the most promising compounds were selected for further assessment of the action and selectivity in the *in vitro* mutant $EGFR^{L858R-TK}$, expressed by IC_{50} (nM), and all tested compounds exhibited good inhibitory activity and closed to Erlotinib as a positive control (IC_{50}= 59.56 nM).

The quinoxaline derivatives **6** demonstrated the strongest of the compounds being tested with IC_{50} (63.70 nM) inhibitory activity of $EGFR^{L858R-TK}$. When bromo-substitution is replaced by chloride as quinoxaline derivative **7b**, the activity decreased to 82.76 nM, which could be due to the difference in the electrostatics between two atoms. Besides, methyl 3-(5-bromo-3-Oxo-3,4-dioquinoxaline-2-yl) propanoate (**7b**) showed moderate activity by IC_{50} (75.42 nM). On the other hand, IC_{50} values (87,34 nM) are identified by the 2-(6-bromo-3-oxo-3,4-dihydroquinoxalin-2(1*H*)-ylidene)acetohydrazide (**3a**).

3.3. In silico *computational analysis studies*

3.3.1. Physicochemical properties and Lipinski's parameters

Physicochemical properties of any molecule significantly affect its bioavailability, absorption, kinetics, and levels of this molecule in different tissues, and all these factors will affect its pharmacological activity. Thus, the most potent anticancer derivatives **3a, 6, 7b**, and **7d** were selected to explore further its molecular properties and Lipinski's parameters (Table 6) using SwissADME [81].

Topological polar surface area (TPSA), solubility, and Lipinski's parameters (Table 6) of the most promising compounds were calculated using SwissADME [81]. PSA is a useful parameter in drug optimization as molecules with a polar surface area value of more than 140 A^2 won't be able to pass through cell membranes [82]. All the most promising compounds showed PSA less than 140 A^2, as shown in Table 6. Lipinski's rule of five (RO5) can help to expect the molecule's oral bioavailability [83]. Our promising derivatives **3a, 6, 7b**, and **7d** showed no violations and all parameters agreed with RO5 (Table 5), and indicate the promiscuity of these derivatives to formulate orally.

3.3.2. Docking study analysis

Our study extended to give a stimulate figure between the newly promising designed compounds **3a, 6, 7b**, and **7d** depending on the Caspases 3, BAX, Bcl-2 and EGFR results, cell cycle, apoptosis inducer, and the selected enzyme. The X-ray structure of EGFR tyrosine kinase co-crystalized with 4-anilinoquinazoline inhibitor (Erlotinib) (PDB code: 1M17) [70,84] was obtained from protein databank (https://www.rcsb.org/). Molecular docking simulation performed by Molecular Operating Environment software 10.2008 (MOE), Chemical Computing Group Inc., Montreal, Quebec, Canada [85]. Docking procedure performed using the standard protocol by generating active site with co-crystallized ligand (Erlotinib). The validation process occurs at the lowest energy to get better results and the solvent molecules were removed according to reported methods [35,46,64]. The obtained data represented in Figs. 7**a-f**.

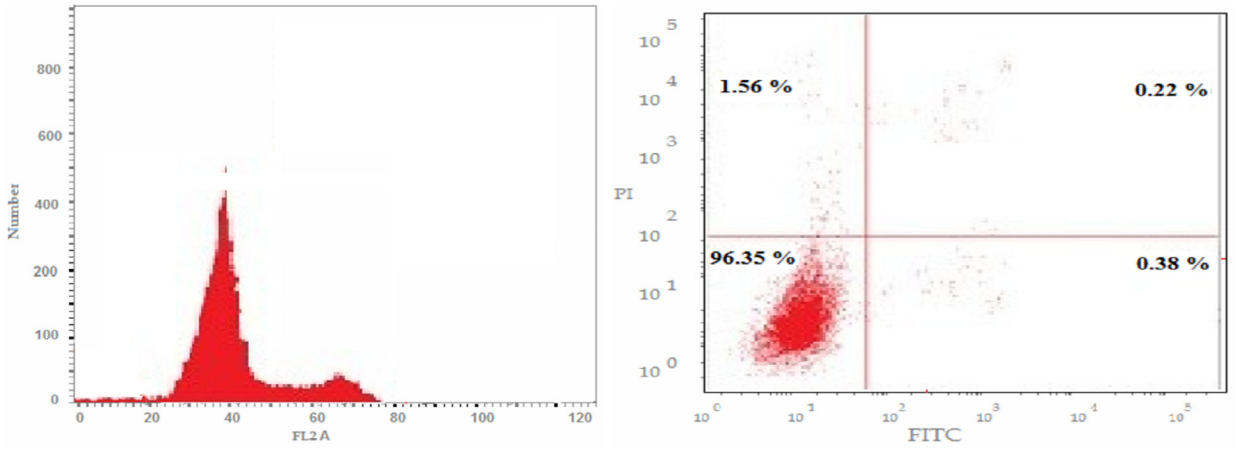

A. Untreated MCF-7

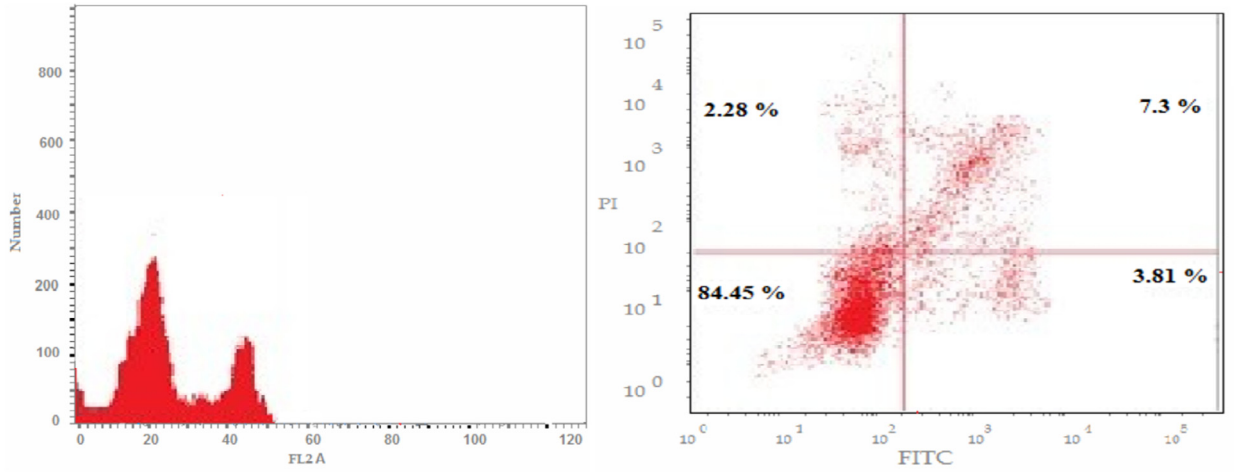

B. 3a/MCF-7

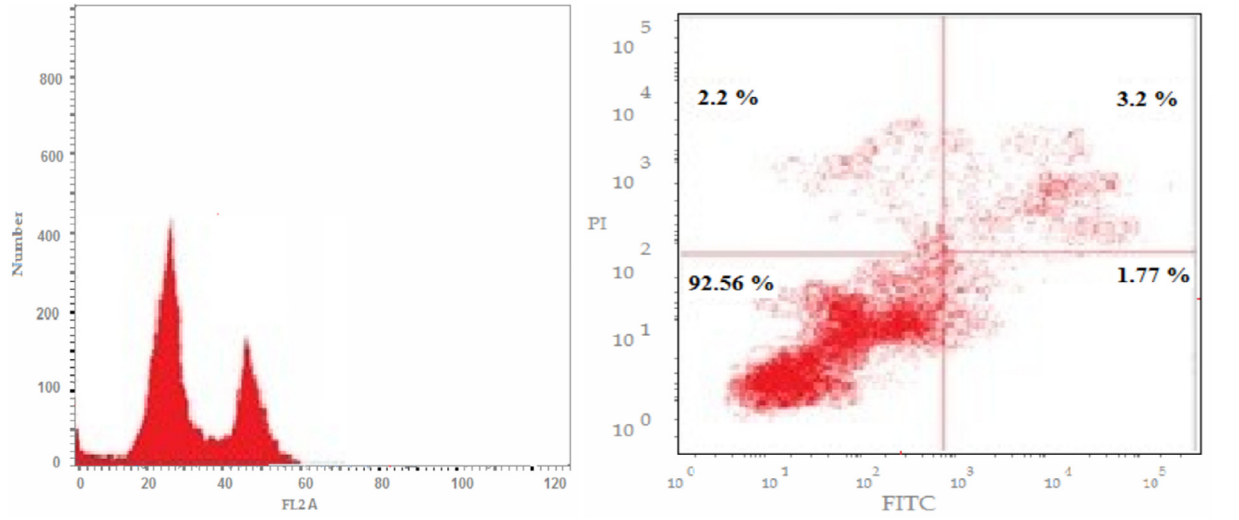

C. 6/MCF-7

Fig. 5. Cell cycle analysis: **A.** Control MCF-7, **B.** Compound **3a, C**. Compound **6, D**. Compound **7b, E**. Compound **7d**, by flow cytometry using PI staining method using10 μM for 24 h.

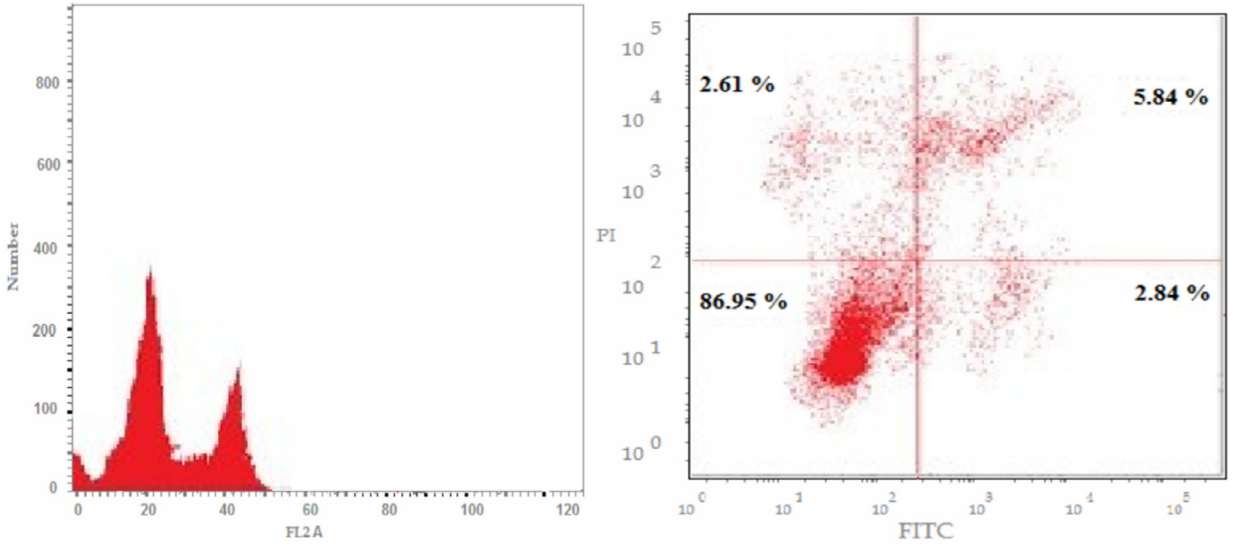

D. 7b/MCF-7

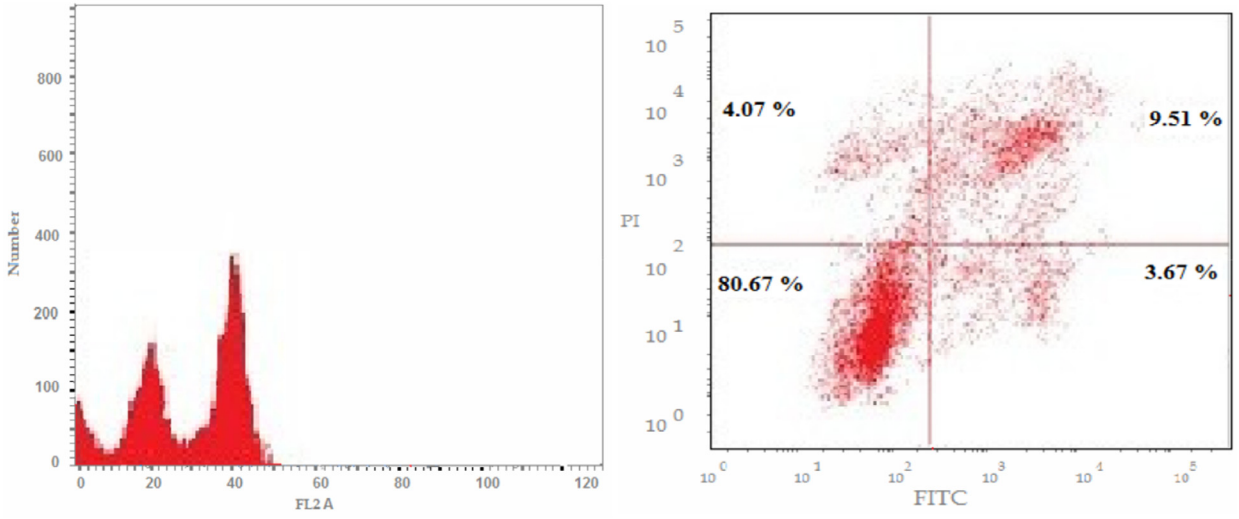

E. 7d/MCF-7

Fig. 5. Continued

Table 6
Solubility, topological surface area and Lipinski's parameters for most promising compounds **3a, 6, 7b, 7d** and **Erlotinib**.

Cpd. No.	Log S (Log moles /L)	TPSA (A^2)	Lipinskiś parameters				
			nHBA (NO)	nHBD (OHNH)	LogP	M.Wt	No. of viol.
3a	-2.23	103.77	3	4	0.61	297.11	0
6	-2.39	52.08	4	0	1.46	200.19	0
7b	-2.63	72.05	4	1	2.64	3.11.13	0
7d	-2.32	72.05	4	1	1.50	266.68	0
Erlotinib	4.11	74.73	6	1	1.89	393.44	0

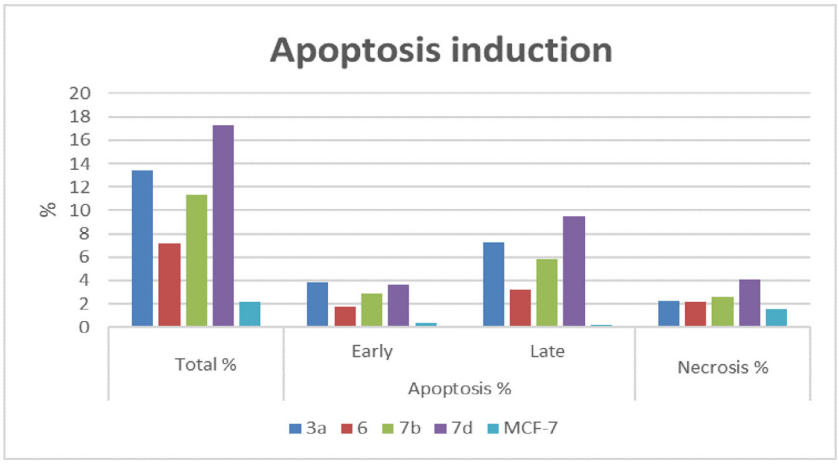

Fig. 6. Percent of cell death induced by compounds **3a, 6, 7b** or **7d** on MCF-7 cells.

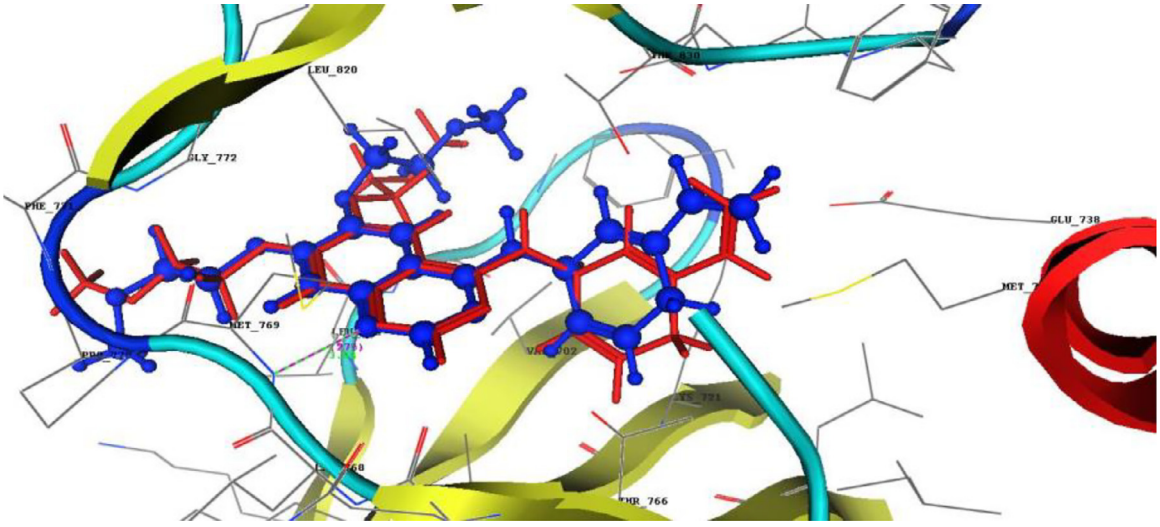

Fig. 7. (a) Superimposition 3D of the co-crystallized (red) and the docking pose (blue) of Erlotinib with RMSD of 1.10 °A in the active site of 1M17. (b) 2D & 3D interactions of original ligand Erlotinib in the active site of 1M17. (c) 2D & 3D interaction maps of compound 3a in the active site of 1M17. (d) 2D & 3D interaction maps of compound 6 in the active site of 1M17. (e) 2D & 3D interaction maps of compound 7b in the active site of 1M17. (f). 2D & 3D interaction maps of compound 7d in the active site of 1M17.

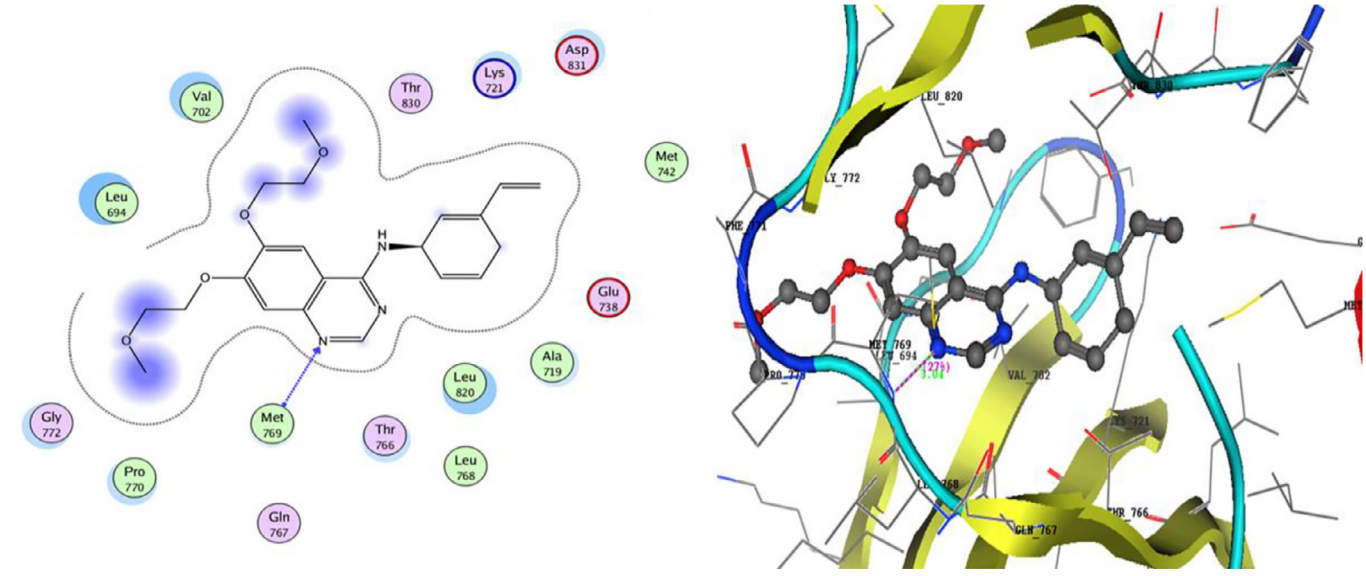

Fig. 7. Continued

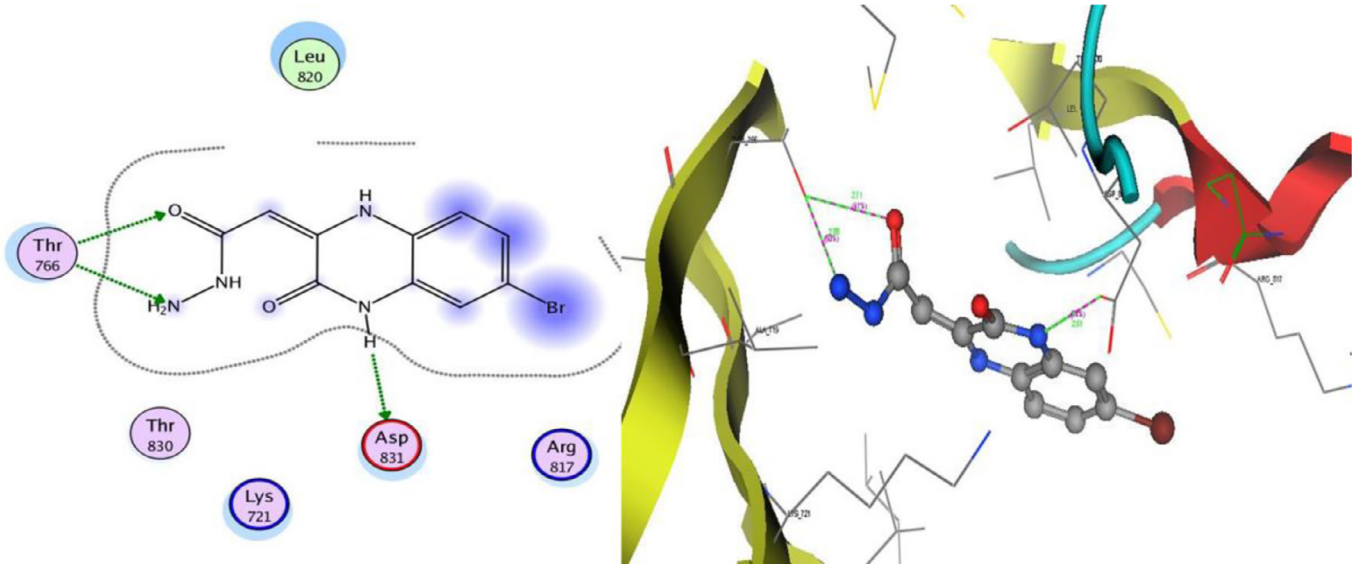

Fig. 7. Continued

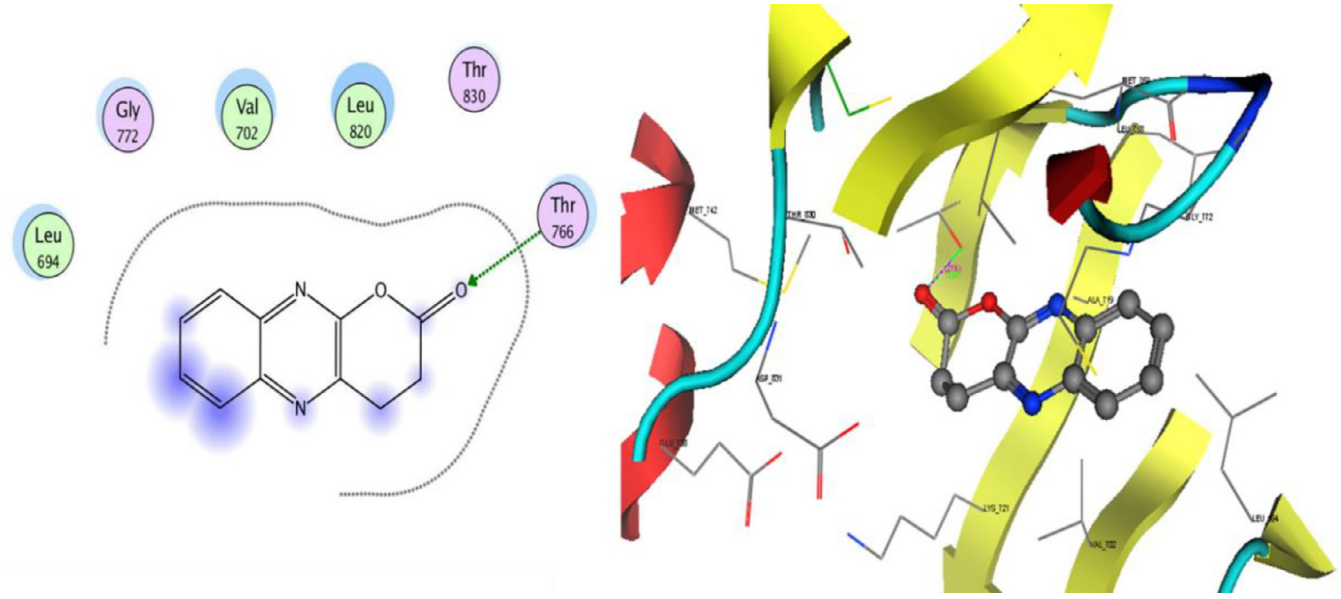

Fig. 7. Continued

The validation process showed that the Erlotinib has an energy score (S)= -17.84 kcal/mol, and RMSD of 1.10 °A, with one H-bond acceptor through Met769 and nitrogen of quinazoline scaffold with bond length (3.04 °A) and strength 27% (Fig. 7a, b). Compound **3a** was found to have docking score energy (S= -16.97 kcal/mol) with two hydrogen bond acceptors from the side chain, between Thr766 and carbonyl of quinoxaline and amino of hydrazide derivative with bond length 2.71, 2.88 °A, and strength 41, 60% respectively. Asp831 and NH of quinoxaline form *H*-bond sidechain donor with bond length 2.51 °A and strength 54% (Fig. 7c). Pyrano[2,3-*b*]quinoxalin-2-one derivatives **6,** displayed score energy (S)= -15.86 kcal/mol that can perform one side chain acceptors through carbonyl of pyran-2-one and Thr766 with bond length 2.93 °A strength 21 % (Fig. 7d).

Compound **7b** with a methyl ester group attached to 6-bromo-3-oxo-3,4-dihydroquinoxalin derivative revealed energy score (S)= -16.95 kcal/mol, as well as one hydrogen bond side chain acceptor between Thr766 and carbonyl of the methyl ester with strength 40 % and bond length 2.58 °A. Furthermore, hydrogen bond backbone acceptor between Met769 and carbonyl of quinoxaline derivative (as an original ligand that forms H-bond with the nitrogen of quinazoline) through bond length 2.68 °A and 48% (Fig. 7e).

Finally, Compound **7d** with methyl ester group attached to 6-chloro-3-oxo-3,4-dihydroquinoxalin derivative showed docking score energy (S= -15.88 kcal/mol), because it forms only one hydrogen bond acceptor between Lys721 and the carbonyl of the methyl ester with bond length 2.56 °A (41%) (Fig. 7f). Moreover, all quinoxaline derivatives **3a, 6, 7b**, and **7d** revealed hydrophobic interaction between amino acids inside the pocket and phenyl derivatives of quinoxaline moiety.

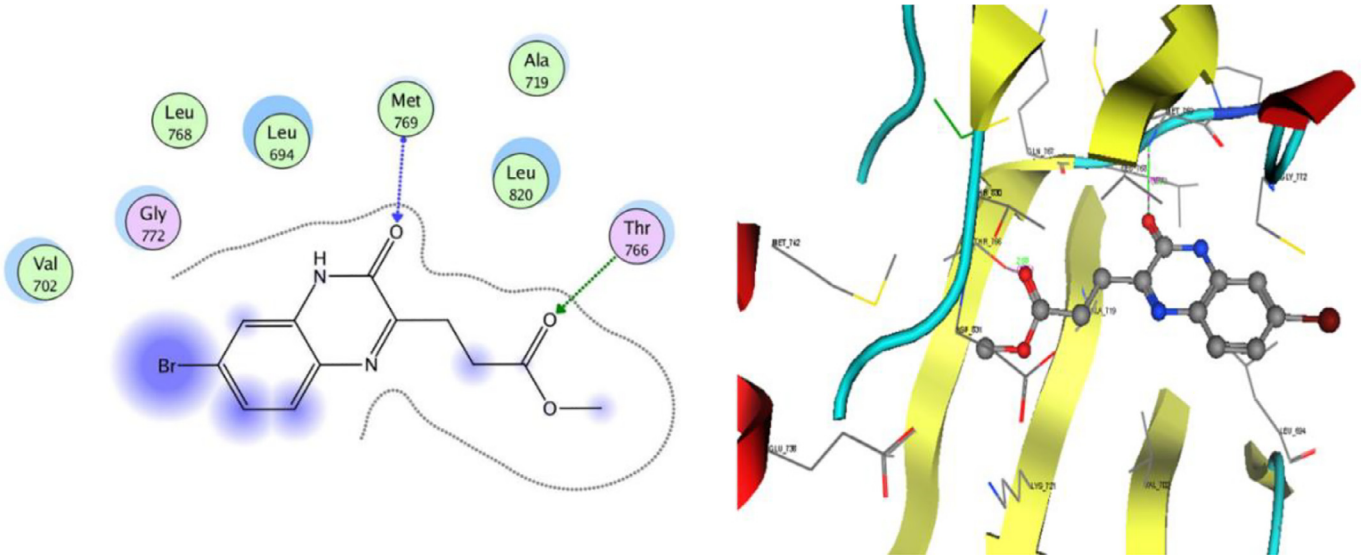

Fig. 7. Continued

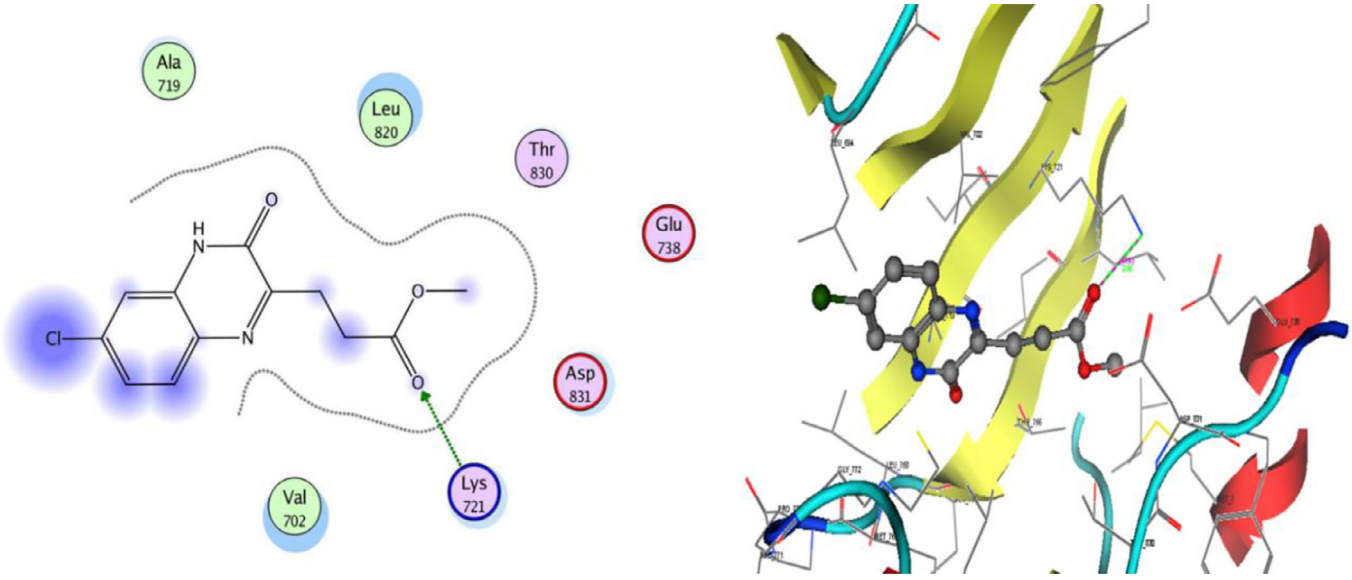

Fig. 7. Continued

4. Conclusion

A novel series of twenty-eight compounds based on quinoxaline nucleus were designed and synthesized. The quinoxaline derivatives were prepared by Cyclo-condensation of 1,2-diaminobenzene derivatives with dimethyl-acetylenedicarboxylate and α-ketoglutaric acid. The obtained quinoxaline derivatives were esterified and reacted with hydrazine to afforded hydrazide derivatives that reacted with an acid chloride, benzaldehyde, and acetophenones derivatives to design new quinoxaline with a new substituent as a side chain. The cytotoxic activities against HepG-2, HCT-116, and MCF-7cell lines were investigated through SRB screening. Most new derivatives exhibited moderate to good *in vitro* anticancer activities, especially against the MCF-7 cell line. The best activities were observed in **3a, 3b, 6, 7b, 7c, 7d** and **7f**. In order to evaluate their apoptotic ability, these compounds have been examined to the apoptosis and observed an increase in the level of apoptosis inducer BAX, caspase-3 activator and a decrease in the expression of the apoptosis suppressor Bcl-2. The cell cycle analysis of the most potent compounds **3a, 6, 7b**, and **7d** revealed that the cell arrest at the G2/M phase ranged between 26.25 % to 48%. The tested derivatives also demonstrated an increase in the amount of pre-G1 phase as a further indication of the apoptosis potential of these derivatives. Additionally, wild $EGFR^{WT}$ and mutant $EGFR^{L858R\text{-}TK}$ inhibitory activity for **3a, 6, 7b**, and **7d** had IC_{50} values ranging from 0.075-1.547 µM versus 63.70-87.34 nM, respectively, and Erlotinib used as a reference standard. Finally, the obtained results are supported by Lipinski's parameters. The promising compounds **3a, 6, 7b**, and **7d** showed no violations, and all parameters agreed with RO5, which indicates promiscuity of these derivatives to formulate orally. The molecular docking simulation showed the docked compounds bounded through different hydrogen bonds inside the active site of (PDB: 1M17), and observed score energy ranged between S (-15.86 to -16.97 kcal/mol) compared to Erlotinib (-17.84 kcal/mol).

Declaration of Competing Interest

The authors declare that they have no known competing financial interests or personal relationships that could have appeared to influence the work reported in this paper.

CRediT authorship contribution statement

Eman A. Fayed: Conceptualization, Methodology, Software, Formal analysis, Validation, Investigation, Data curation, Supervision, Writing - original draft, Writing - review & editing. **Yousry A. Ammar:** Conceptualization, Methodology, Formal analysis, Investigation, Resources, Writing - original draft, Supervision, Project administration. **Marwa A. Saleh:** Conceptualization, Methodology, Investigation, Resources, Writing - original draft. **Ashraf H. Bayoumi:** Conceptualization, Resources, Writing - original draft, Supervision. **Amany Belal:** Methodology. **Ahmed B.M. Mehany:** Methodology. **Ahmed Ragab:** Conceptualization, Software, Formal analysis, Validation, Methodology, Investigation, Data curation, Writing - original draft, Writing - review & editing, Visualization.

References

[1] R.L. Siegel, K.D. Miller, A. Jemal, Cancer statistics, 2016, CA. Cancer J. Clin. 66 (2016) 7–30, doi:10.3322/caac.21332.

[2] W. Gu, S. Wang, X. Jin, Y. Zhang, D. Hua, T. Miao, X. Tao, S. Wang, Synthesis and Evaluation of New Quinoxaline Derivatives of Dehydroabietic Acid as Potential Antitumor Agents, Mol. . 22 (2017). doi:10.3390/molecules22071154.

[3] İ. Işıkdağ, Y. Özkay, H.T. Karakoç, Synthesis and anticancer activity of some bisquinoxaline derivatives, 2011.

[4] J. Caballero, M. Fernández, Artificial neural networks from MATLAB® in medicinal chemistry. Bayesian-regularized genetic neural networks (BRGNN): Application to the prediction of the antagonistic activity against human platelet thrombin receptor (PAR-1), Curr. Top. Med. Chem. 8 (2008) 1580–1605.

[5] V.S. Parmar, N.K. Sharma, M. Husain, A.C. Watterson, J. Kumar, L.A. Samuelson, A.L. Cholli, A.K. Prasad, A. Kumar, S. Malhotra, N. Kumar, A. Jha, A. Singh, I. Singh, A.Vats Himanshu, N.A. Shakil, S. Trikha, S. Mukherjee, S.K. Sharma, S.K. Singh, A. Kumar, H.N. Jha, C.E. Olsen, C.P. Stove, M.E. Bracke, M.M. Mareel, Synthesis, characterization and in vitro anti-invasive activity screening of polyphenolic and heterocyclic compounds, Bioorg. Med. Chem. 11 (2003) 913–929, doi:10.1016/S0968-0896(02)00539-4.

[6] K. Šavikin, G. Zdunić, T. Janković, T. Stanojković, Z. Juranić, N. Menković, In vitro cytotoxic and antioxidative activity of Cornus mas and Cotinus coggygria, Nat. Prod. Res. 23 (2009) 1731–1739, doi:10.1080/14786410802267650.

[7] R. Filosa, A. Peduto, P. de Caprariis, C. Saturnino, M. Festa, A. Petrella, A. Pau, G.A. Pinna, P.La Colla, B. Busonera, R. Loddo, Synthesis and antiproliferative properties of N3/8-disubstituted 3,8-diazabicyclo[3.2.1]octane analogues of 3,8-bis[2-(3,4,5-trimethoxyphenyl)pyridin-4-yl]methyl-piperazine, Eur. J. Med. Chem. 42 (2007) 293–306, doi:10.1016/j.ejmech.2006.11.013.

[8] H.W. Findley, L. Gu, A.M. Yeager, M. Zhou, Expression and Regulation of Bcl-2, Bcl-xl, and Bax Correlate With p53 Status and Sensitivity to Apoptosis in Childhood Acute Lymphoblastic Leukemia, Blood 89 (1997) 2986–2993, doi:10.1182/blood.V89.8.2986.

[9] D.E. Fisher, Apoptosis in cancer therapy: crossing the threshold, Cell 78 (1994) 539–542.

[10] Z.N. Oltval, C.L. Milliman, S.J. Korsmeyer, Bcl-2 heterodimerizes in vivo with a conserved homolog, Bax, that accelerates programed cell death, Cell 74 (1993) 609–619, doi:10.1016/0092-8674(93)90509-O.

[11] T. Narisawa, Y. Fukaura, K. Yazawa, C. Ishikawa, Y. Isoda, Y. Nishizawa, Colon cancer prevention with a small amount of dietary perilla oil high in alpha-linolenic acid in an animal model, Cancer 73 (1994) 2069–2075. doi:10.1002/1097-0142(19940415)73:8<2069::AID-CNCR2820730810>3.0.CO;2-1.

[12] D. Singh, B.K. Attri, R.K. Gill, J. Bariwal, Review on EGFR inhibitors: critical updates, Mini Rev. Med. Chem. 16 (2016) 1134–1166.

[13] S.A. Galal, A.S. Abdelsamie, S.M. Soliman, J. Mortier, G. Wolber, M.M. Ali, H. Tokuda, N. Suzuki, A. Lida, R.A. Ramadan, H.I. El Diwani, Design, synthesis and structure–activity relationship of novel quinoxaline derivatives as cancer chemopreventive agent by inhibition of tyrosine kinase receptor, Eur. J. Med. Chem. 69 (2013) 115–124, doi:10.1016/j.ejmech.2013.07.049.

[14] S.T. Hazeldine, L. Polin, J. Kushner, K. White, T.H. Corbett, J. Biehl, J.P. Horwitz, Part 3: Synthesis and biological evaluation of some analogs of the antitumor agents, 2-{4-[(7-chloro-2-quinoxalinyl)oxy]phenoxy}propionic acid, and 2-{4-[(7-bromo-2-quinolinyl)oxy]phenoxy}propionic acid, Bioorg. Med. Chem. 13 (2005) 1069–1081, doi:10.1016/j.bmc.2004.11.034.

[15] S.T. Hazeldine, L. Polin, J. Kushner, K. White, N.M. Bouregeois, B. Crantz, E. Palomino, T.H. Corbett, J.P. Horwitz, II. Synthesis and Biological Evaluation of Some Bioisosteres and Congeners of the Antitumor Agent, 2-{4-[(7-Chloro-2-quinoxalinyl)oxy]phenoxy}propionic Acid (XK469), J. Med. Chem. 45 (2002) 3130–3137, doi:10.1021/jm0200097.

[16] S.T. Hazeldine, L. Polin, J. Kushner, J. Paluch, K. White, M. Edelstein, E. Palomino, T.H. Corbett, J.P. Horwitz, Design, Synthesis, and Biological Evaluation of Analogues of the Antitumor Agent, 2-{4-[(7-Chloro-2-quinoxalinyl)oxy]phenoxy}propionic Acid (XK469), J. Med. Chem. 44 (2001) 1758–1776, doi:10.1021/jm0005149.

[17] M.M. El-Enany, M.M. Kamel, O.M. Khalil, H.B. El-Nassan, Synthesis and antitumor activity of novel 6-aryl and 6-alkylpyrazolo[3,4-d]pyrimidin-4-one derivatives, Eur. J. Med. Chem. 45 (2010) 5286–5291, doi:10.1016/j.ejmech.2010.08.048.

[18] H.E.A. Ahmed, S.K. Ihmaid, A.M. Omar, A.M. Shehata, H.S. Rateb, M.F. Zayed, S. Ahmed, M.M. Elaasser, Design, synthesis, molecular docking of new lipophilic acetamide derivatives affording potential anticancer and antimicrobial agents, Bioorg. Chem. 76 (2018) 332–342, doi:10.1016/j.bioorg.2017.11.019.

[19] B. Dietrich, U. Diederichsen, Synthesis of Cyclopeptidic Analogues of Triostin A with Quinoxalines or Nucleobases as Chromophores, European J. Org. Chem. 2005 (2005) 147–153, doi:10.1002/ejoc.200400548.

[20] A. Basak, H. Dugas, Design and synthesis of DNA intercalating crown ether molecules, Tetrahedron Lett 27 (1986) 3–6, doi:10.1016/S0040-4039(00)83924-6.

[21] A. Dell, D.H. Williams, H.R. Morris, G.A. Smith, J. Feeney, G.C.K. Roberts, Structure revision of the antibiotic echinomycin, J. Am. Chem. Soc. 97 (1975) 2497–2502, doi:10.1021/ja00842a029.

[22] H.T. Cheung, J. Feeney, G.C.K. Roberts, D.H. Williams, G. Ughetto, M.J. Waring, The conformation of echinomycin in solution, J. Am. Chem. Soc. 100 (1978) 46–54, doi:10.1021/ja00469a008.

[23] M.J. Waring, L.P.G. Wakelin, Echinomycin: a bifunctional intercalating antibiotic, Nature 252 (1974) 653–657, doi:10.1038/252653a0.

[24] J.R. Rigas, W.P. Tong, M.G. Kris, J.P. Orazem, C.W. Young, R.P. Warrell, Phase I Clinical and Pharmacological Study of Chloroquinoxaline Sulfonamide, Cancer Res 52 (1992) 6619 LP–6623 http://cancerres.aacrjournals.org/content/52/23/6619.abstract .

[25] Z. Ding, R.E. Parchment, P.M. LoRusso, J.-Y. Zhou, J. Li, T.S. Lawrence, Y. Sun, G.S. Wu, The Investigational New Drug XK469 Induces G₂-M Cell Cycle Arrest by p53-dependent and -independent Pathways, Clin. Cancer Res. 7 (2001) 3336 LP –3342 http://clincancerres.aacrjournals.org/content/7/11/3336.abstract .

[26] S. Tanimori, T. Nishimura, M. Kirihata, Synthesis of novel quinoxaline derivatives and its cytotoxic activities, Bioorg. Med. Chem. Lett. 19 (2009) 4119–4121, doi:10.1016/j.bmcl.2009.06.007.

[27] R.E. TenBrink, W.B. Im, V.H. Sethy, A.H. Tang, D.B. Carter, Antagonist, Partial Agonist, and Full Agonist Imidazo[1,5-a]quinoxaline Amides and Carbamates Acting through the GABAA/Benzodiazepine Receptor, J. Med. Chem. 37 (1994) 758–768, doi:10.1021/jm00032a008.

[28] D.-S. Su, M.K. Markowitz, R.M. DiPardo, K.L. Murphy, C.M. Harrell, S.S. O'Malley, R.W. Ransom, R.S.L. Chang, S. Ha, F.J. Hess, D.J. Pettibone, G.S. Mason, S. Boyce, R.M. Freidinger, M.G. Bock, Discovery of a Potent, Non-peptide Bradykinin B1 Receptor Antagonist, J. Am. Chem. Soc. 125 (2003) 7516–7517, doi:10.1021/ja0353457.

[29] Y.A. Ammar, A.A. Farag, A.M. Ali, A. Ragab, A.A. Askar, D.M. Elsisi, A. Belal, Design, synthesis, antimicrobial activity and molecular docking studies of some novel di-substituted sulfonylquinoxaline derivatives, Bioorg. Chem. 104 (2020) 104164, doi:10.1016/j.bioorg.2020.104164.

[30] N. Kumar, P. Sharma, N. Kaur, A. Pareek, An Efficient synthesis and Biological activity of Quinoxaline-2-Carboxylic acid and its derivatives, J. Appl. Chem. 2 (2013) 143–149.

[31] C.E. Voogd, J.J. van der Stel, J.J.J.A.A. Jacobs, The mutagenic action of quindoxin, carbadox, olaquindox and some other N-oxides on bacteria and yeast, Mutat. Res. Toxicol. 78 (1980) 233–242, doi:10.1016/0165-1218(80)90104-4.

[32] Y.A. Ammar, A.M. El-Sharief, Y.A. Mohamed, A.B. Mehany, A. Ragab, Synthesis, spectral characterization and pharmacological evaluation of novel thiazole-oxoindole hybrid compounds as potential anticancer agents, Al-Azhar Bull. Sci. 29 (2018) 25–37, doi:10.21608/absb.2018.33767.

[33] S.A. Galal, K.H. Hegab, A.S. Kassab, M.L. Rodriguez, S.M. Kerwin, A.-M.A. El-Khamry, H.I. El Diwani, New transition metal ion complexes with benzimidazole-5-carboxylic acid hydrazides with antitumor activity, Eur. J. Med. Chem. 44 (2009) 1500–1508, doi:10.1016/j.ejmech.2008.07.013.

[34] É. Csikós, C. Gönczi, B. Podányi, G. Tóth, I. Hermecz, Regioselectivity in preparation of unsymmetrically substituted 3-aminoquinoxalin-2(1H)-ones, J. Chem. Soc.{,} Perkin Trans. 1. (1999) 1789–1794, doi:10.1039/A902978H.

[35] Y.A. Ammar, A.M. Sh. El-Sharief, A. Belal, S.Y. Abbas, Y.A. Mohamed, A.B.M. Mehany, A. Ragab, Design, synthesis, antiproliferative activity, molecular docking and cell cycle analysis of some novel (morpholinosulfonyl) isatins with potential EGFR inhibitory activity, Eur. J. Med. Chem. 156 (2018) 918–932, doi:10.1016/j.ejmech.2018.06.061.

[36] D. Kumar, V. Judge, R. Narang, S. Sangwan, E. De Clercq, J. Balzarini, B. Narasimhan, Benzylidene/2-chlorobenzylidene hydrazides: Synthesis, antimicrobial activity, QSAR studies and antiviral evaluation, Eur. J. Med. Chem. 45 (2010) 2806–2816, doi:10.1016/j.ejmech.2010.03.002.

[37] N.C. Romeiro, G. Aguirre, P. Hernández, M. González, H. Cerecetto, I. Aldana, S. Pérez-Silanes, A. Monge, E.J. Barreiro, L.M. Lima, Synthesis, trypanocidal activity and docking studies of novel quinoxaline-N-acylhydrazones, designed as cruzain inhibitors candidates, Bioorg. Med. Chem. 17 (2009) 641–652, doi:10.1016/j.bmc.2008.11.065.

[38] L. Huang, L.S. Brinen, J.A. Ellman, Crystal structures of reversible ketone-Based inhibitors of the cysteine protease cruzain, Bioorg. Med. Chem. 11 (2003) 21–29, doi:10.1016/S0968-0896(02)00427-3.

[39] C.D. Duarte, E.J. Barreiro, C.A.M. Fraga, Privileged Structures: A Useful Concept for the Rational Design of New Lead Drug Candidates, Mini Rev. Med. Chem. 7 (n.d.) 1108–1119. https://www.ingentaconnect.com/content/ben/mrmc/2007/00000007/00000011/art00003.

[40] F.A.R. Rodrigues, I. da S. Bomfim, B.C. Cavalcanti, C. do Ó. Pessoa, J.L. Wardell, S.M.S.V Wardell, A.C. Pinheiro, C.R. Kaiser, T.C.M. Nogueira, J.N. Low, L.R. Gomes, M.V.N. de Souza, Design, synthesis and biological evaluation of (E)-2-(2-arylhydrazinyl)quinoxalines, a promising and potent new class of anticancer agents, Bioorg. Med. Chem. Lett. 24 (2014) 934–939, doi:10.1016/j.bmcl.2013.12.074.

[41] S. ElKalyoubi, E. Fayed, Synthesis and Evaluation of Antitumour Activities of Novel Fused Tri- and Tetracyclic Uracil Derivatives, J. Chem. Res. 40 (2016) 771–777. doi:10.3184/174751916×14798125870610.

[42] E.A. Fayed, S.I. Eissa, A.H. Bayoumi, N.A. Gohar, A.B.M. Mehany, Y.A. Ammar, Design, synthesis, cytotoxicity and molecular modeling studies of some novel fluorinated pyrazole-based heterocycles as anticancer and apoptosis-inducing agents, Mol. Divers. 23 (2019) 165–181, doi:10.1007/s11030-018-9865-9.

[43] E.A. Fayed, R. Sabour, M.F. Harras, A.B.M. Mehany, Design, synthesis, biological evaluation and molecular modeling of new coumarin derivatives as potent anticancer agents, Med. Chem. Res. 28 (2019) 1284–1297, doi:10.1007/s00044-019-02373-x.

[44] M.M.F. Ismail, K.M. Amin, E. Noaman, D.H. Soliman, Y.A. Ammar, New quinoxaline 1, 4-di-N-oxides: Anticancer and hypoxia-selective therapeutic agents, Eur. J. Med. Chem. 45 (2010) 2733–2738, doi:10.1016/j.ejmech.2010.02.052.

[45] H.F. Rizk, M.A. El-Borai, A. Ragab, S.A. Ibrahim, Design, synthesis, biological evaluation and molecular docking study based on novel fused pyrazolothiazole scaffold, J. Iran. Chem. Soc. (2020), doi:10.1007/s13738-020-01944-9.

[46] M.A. Salem, A. Ragab, A. El-Khalafawy, A.H. Makhlouf, A.A. Askar, Y.A. Ammar, Design, synthesis, in vitro antimicrobial evaluation and molecular docking studies of indol-2-one tagged with morpholinosulfonyl moiety as DNA gyrase inhibitors, Bioorg. Chem. 96 (2020) 103619, doi:10.1016/j.bioorg.2020.103619.

[47] M.A. Salem, A. Ragab, A.A. Askar, A. El-Khalafawy, A.H. Makhlouf, One-pot synthesis and molecular docking of some new spiropyranindol-2-one derivatives as immunomodulatory agents and in vitro antimicrobial potential with DNA gyrase inhibitor, Eur. J. Med. Chem. 188 (2020) 111977, doi:10.1016/j.ejmech.2019.111977.

[48] M.A.M.S. El-Sharief, S.Y. Abbas, M.A. Zahran, Y.A. Mohamed, A. Ragab, Y.A. Ammar, New 1, 3-diaryl-5-thioxo-imidazolidin-2, 4-dione derivatives: Synthesis, reactions and evaluation of antibacterial and antifungal activities, Zeitschrift Fur Naturforsch. - Sect. B J. Chem. Sci. 71 (2016), doi:10.1515/znb-2016-0054.

[49] Y.A. Ammar, S.Y. Abbas, M.A.M.S. El-Sharief, M.A.E.-R. Salem, A.R. Mohamed, Synthesis and characterization of new imidazolidineiminothione and bis-imidazolidineiminothione derivatives as potential antimicrobial agents, Eur. J. Chem. 8 (2017) 76–81, doi:10.5155/eurjchem.8.1.76-81.1542.

[50] Y.A. Ammar, A.A. Farag, A.M. Ali, S.A. Hessein, A.A. Askar, E.A. Fayed, D.M. Elsisi, A. Ragab, Antimicrobial evaluation of thiadiazino and thiazolo quinoxaline hybrids as potential DNA gyrase inhibitors; design, synthesis, characterization and morphological studies, Bioorg. Chem. 99 (2020) 103841, doi:10.1016/j.bioorg.2020.103841.

[51] Y.A. Ammar, M.A.M.S. El-Sharief, M.M. Ghorab, Y.A. Mohamed, A. Ragab, S.Y. Abbas, New imidazolidineiminothione, imidazolidin-2-one and imidazoquinoxaline derivatives: Synthesis and evaluation of antibacterial and antifungal activities, Curr. Org. Synth. (2016) 13.

[52] K.M. Amin, M.M.F. Ismail, E. Noaman, D.H. Soliman, Y.A. Ammar, New quinoxaline 1,4-di-N-oxides. Part 1: Hypoxia-selective cytotoxins and anticancer agents derived from quinoxaline 1,4-di-N-oxides, Bioorg. Med. Chem. 14 (2006) 6917–6923, doi:10.1016/j.bmc.2006.06.038.

[53] A.R. Al-Marhabi, H.-A.S. Abbas, Y.A. Ammar, Synthesis, Characterization and Biological Evaluation of Some Quinoxaline Derivatives: A Promising and Potent New Class of Antitumor and Antimicrobial Agents, Mol 20 (2015), doi:10.3390/molecules201119655.

[54] H.-A.S. Abbas, A.R.M. Al-Marhabi, Y.A. Ammar, Design, synthesis and biological evaluation of 2, 3-disubstituted and fused quinoxalines as potential anticancer and antimicrobial agents, Acta Pol. Pharm. 74 (2017) 445–458.

[55] A. Ragab, S.A. Fouad, O.A.A. Ali, E.M. Ahmed, A.M. Ali, A.A. Askar, Y.A. Ammar, Sulfaguanidine Hybrid with Some New Pyridine-2-One Derivatives: Design, Synthesis, and Antimicrobial Activity against Multidrug-Resistant Bacteria as Dual DNA Gyrase and DHFR Inhibitors, Antibiotics 10 (2021) 162, doi:10.3390/antibiotics10020162.

[56] M.M.S. Wassel, W.M. Gamal Eldin, A. Ragab, G.A.M. Elhag Ali, Y.A. Ammar, Antiviral Activity Of Adamantane-Pyrazole Derivatives Against Foot And Mouth Disease Virus Infection In Vivo And In Vitro With Molecular Docking Study, J. Appl. Vet. Sci. 5 (2020) 37–46, doi:10.21608/javs.2020.118001.

[57] O.O. Ajani, C.A. Obafemi, O.C. Nwinyi, D.A. Akinpelu, Microwave assisted synthesis and antimicrobial activity of 2-quinoxalinone-3-hydrazone derivatives, Bioorg. Med. Chem. 18 (2010) 214–221, doi:10.1016/j.bmc.2009.10.064.

[58] S. Tariq, O. Alam, M. Amir, Synthesis, anti-inflammatory, p38α MAP kinase inhibitory activities and molecular docking studies of quinoxaline derivatives containing triazole moiety, Bioorg. Chem. 76 (2018) 343–358, doi:10.1016/j.bioorg.2017.12.003.

[59] R.J. Harding, R. Ferreira de Freitas, P. Collins, I. Franzoni, M. Ravichandran, H. Ouyang, K.A. Juarez-Ornelas, M. Lautens, M. Schapira, F. von Delft, V. Santhakumar, C.H. Arrowsmith, Small Molecule Antagonists of the Interaction between the Histone Deacetylase 6 Zinc-Finger Domain and Ubiquitin, J. Med. Chem. 60 (2017) 9090–9096, doi:10.1021/acs.jmedchem.7b00933.

[60] Y. Cheng, T. Powers, K. Ashton, J. Brown, S. Harried, S.A. Hitchcock, T. Judd, P. Lopez, T. Nixey, N.A. Paras, Amino heteroaryl compounds as beta-secretase modulators and methods of use, (2016).

[61] Y. Deepika, P.S. Nath, Design, Synthesis of Novel Quinoxaline Derivatives and their Antinociceptive Activity, Asian J. Pharm. Heal. Sci. 2 (2012).

[62] V. Vichai, K. Kirtikara, Sulforhodamine B colorimetric assay for cytotoxicity screening, Nat. Protoc. 1 (2006) 1112–1116, doi:10.1038/nprot.2006.179.

[63] N. Elmadany, E. Khalil, L. Vaccari, G. Birarda, I. Yousef, R. Abu-Dahab, Antiproliferative activity of the combination of doxorubicin/quercetin on MCF7 breast cancer cell line: A combined study using colorimetric assay and synchrotron infrared microspectroscopy, Infrared Phys. Technol. 95 (2018) 141–147, doi:10.1016/j.infrared.2018.10.014.

[64] A.M.S. El-sharief, Y.A. Ammar, A. Belal, M.A.M.S. El-sharief, Y.A. Mohamed, A.B.M. Mehany, G.A.M. Elhag, A. Ragab, Design, synthesis, molecular docking and biological activity evaluation of some novel indole derivatives as potent anticancer active agents and apoptosis inducers, Bioorg. Chem. 85 (2019) 399–412, doi:10.1016/j.bioorg.2019.01.016.

[65] M.A.H. Zahran, B. El-Aarag, A.B.M. Mehany, A. Belal, A.S. Younes, Design, synthesis, biological evaluations, molecular docking, and in vivo studies of novel phthalimide analogs, Arch. Pharm. (Weinheim). 351 (2018) 1700363, doi:10.1002/ardp.201700363.

[66] K.K.-W. Lo, T.K.-M. Lee, J.S.-Y. Lau, W.-L. Poon, S.-H. Cheng, Luminescent biological probes derived from ruthenium(II) estradiol polypyridine complexes, Inorg. Chem. 47 (2008) 200–208, doi:10.1021/ic701735q.

[67] Y. Zhou, H.-Y. Zhao, K.-L. Han, Y. Yang, B.-B. Song, Q.-N. Guo, Z.-C. Fan, Y.-M. Zhang, Y.-O. Teng, P. Yu, 5-(2-Carboxyethenyl) isatin derivative induces G2/M cell cycle arrest and apoptosis in human leukemia K562 cells, Biochem. Biophys. Res. Commun. 450 (2014) 1650–1655, doi:10.1016/j.bbrc.2014.07.053.

[68] F. Manetti, G.A. Locatelli, G. Maga, S. Schenone, M. Modugno, S. Forli, F. Corelli, M. Botta, A combination of docking/dynamics simulations and pharmacophoric modeling to discover new dual c-Src/Abl kinase inhibitors, J. Med. Chem. 49 (2006) 3278–3286.

[69] Y. Jia, C.M. Quinn, A.I. Gagnon, R. Talanian, Homogeneous time-resolved fluorescence and its applications for kinase assays in drug discovery, Anal. Biochem. 356 (2006) 273–281.

[70] Protein data bank, (n.d.) https://www.rcsb.org/structure/1M17 ; last access.

[71] A.S. Hassan, A.A. Askar, A.M. Naglah, A.A. Almehizia, A. Ragab, Discovery of New Schiff Bases Tethered Pyrazole Moiety: Design, Synthesis, Biological Evaluation, and Molecular Docking Study as Dual Targeting DHFR/DNA Gyrase Inhibitors with Immunomodulatory Activity, Mol 25 (2020), doi:10.3390/molecules25112593.

[72] G. Choudhary, R.K. Peddinti, Introduction of a clean and promising protocol for the synthesis of β-amino-acrylates and 1,4-benzoheterocycles: an emerging innovation, Green Chem 13 (2011) 3290–3299, doi:10.1039/C1GC15701A.

[73] E.A. Fayed, Y.A. Ammar, A. Ragab, N.A. Gohar, A.B.M. Mehany, A.M. Farrag, In vitro cytotoxic activity of thiazole-indenoquinoxaline hybrids as apoptotic agents, design, synthesis, physicochemical and pharmacokinetic studies, Bioorg. Chem. 100 (2020) 103951, doi:10.1016/j.bioorg.2020.103951.

[74] M.M.S. Wassel, A. Ragab, G.A.M. Elhag Ali, A.B.M. Mehany, Y.A. Ammar, Novel adamantane-pyrazole and hydrazone hybridized: design, synthesis, cytotoxic evaluation, SAR study and molecular docking simulation as carbonic anhydrase inhibitors, J. Mol. Struct. 1223 (2021) 128966, doi:10.1016/j.molstruc.2020.128966.

[75] P. Limpachayaporn, M. Schäfers, O. Schober, K. Kopka, G. Haufe, Synthesis of new fluorinated, 2-substituted 5-pyrrolidinylsulfonyl isatin derivatives as caspase-3 and caspase-7 inhibitors: Nonradioactive counterparts of putative PET-compatible apoptosis imaging agents, Bioorg. Med. Chem. 21 (2013) 2025–2036, doi:10.1016/j.bmc.2013.01.011.

[76] M. Tavari, S.F. Malan, J. Joubert, Design, synthesis, biological evaluation and docking studies of sulfonyl isatin derivatives as monoamine oxidase and caspase-3 inhibitors, Medchemcomm 7 (2016) 1628–1639, doi:10.1039/C6MD00228E.

[77] H. Jiang, P. Zhao, D. Su, J. Feng, S. Ma, Paris saponin I induces apoptosis via increasing the Bax/Bcl–2 ratio and caspase–3 expression in gefitinib–resistant non–small cell lung cancer in vitro and in vivo, Mol. Med. Rep. 9 (2014) 2265–2272.

[78] R.J. Youle, A. Strasser, The BCL-2 protein family: opposing activities that mediate cell death, Nat. Rev. Mol. Cell Biol. 9 (2008) 47–59, doi:10.1038/nrm2308.

[79] C.K. Tang, Role of Epidermal Growth Factor Receptor in Breast Carcinoma, Handb. Immunohistochem. Situ Hybrid, Hum. Carcinomas Mol. Genet. Lung Breast Carcinomas. 1 (2004) 415, doi:10.1016/S1874-5784(04)80052-7.

[80] Y. Hao, J. Lyu, R. Qu, Y. Tong, D. Sun, F. Feng, L. Tong, T. Yang, Z. Zhao, L. Zhu, J. Ding, Y. Xu, H. Xie, H. Li, Design, Synthesis, and Biological Evaluation of Pyrimido[4,5-d]pyrimidine-2,4(1H,3H)-diones as Potent and Selective Epidermal Growth Factor Receptor (EGFR) Inhibitors against L858R/T790M Resistance Mutation, J. Med. Chem. 61 (2018) 5609–5622, doi:10.1021/acs.jmedchem.8b00346.

[81] http://swissadme.ch/index.php; last access 4/5/2020.

[82] H. Pajouhesh, G.R. Lenz, Medicinal chemical properties of successful central nervous system drugs, NeuroRX 2 (2005) 541–553, doi:10.1602/neurorx.2.4.541.

[83] C.A. Lipinski, F. Lombardo, B.W. Dominy, P.J. Feeney, Experimental and computational approaches to estimate solubility and permeability in drug discovery and development settings, Adv. Drug Deliv. Rev. 23 (1997) 3–25, doi:10.1016/S0169-409X(96)00423-1.

[84] M.M.S. Wassel, Y.A. Ammar, G.A.M. Elhag Ali, A. Belal, A.B.M. Mehany, A. Ragab, Development of adamantane scaffold containing 1,3,4-thiadiazole derivatives: Design, synthesis, anti-proliferative activity and molecular docking study targeting EGFR, Bioorg. Chem. 110 (2021) 104794 In press, doi:10.1016/j.bioorg.2021.104794.

[85] S.I. Eissa, A.M. Farrag, S.Y. Abbas, M.F. El Shehry, A. Ragab, E.A. Fayed, Y.A. Ammar, Novel structural hybrids of quinoline and thiazole moieties: Synthesis and evaluation of antibacterial and antifungal activities with molecular modeling studies, Bioorg. Chem. 110 (2021) 104803 In press, doi:10.1016/j.bioorg.2021.104803.